DESIGN OF SIX COMPONENT FORCE AND MOMENT SENSOR FOR WIND TUNNEL TEST

HABTAMU MAMO YIMAM

Thesis submitted to Mechanical Engineering Department

Presented in partial fulfillment of the requirements for the

Degree of Master of Science in Mechanical Engineering

(Mechanical Design)

Addis Ababa University, Institute of Technology

Addis Ababa, Ethiopia

February 2013

Addis Ababa University

Institute of Technology

This is to certify that the thesis prepared by Habtamu Mamo, entitled: Design of six component force and moment sensor for wind tunnel test and submitted in partial fulfillment of the requirements for the degree of Master of Science (Mechanical Design) compiles with the regulations of the University and meets the accepted standards with respect to originality and quality.

Signed by the Examining committee:

Examiner _____ Signature _____ Date _____

Examiner _____ Signature _____ Date _____

Adviser _____ Signature _____ Date _____

Adviser _____ Signature _____ Date _____

_____

Chair of Department or Graduate Program Coordinator

Abstract

Design of Six Component Force and Moment Sensor for Wind Tunnel Test

This study describes the development of a new six component force and moment sensor using a rectangular box like structure, which can be used to measure aerodynamic forces F_x, F_y and F_z and moments M_x, M_y and M_z simultaneously in wind tunnel. An inbuilt cantilever beams are used as a sensing element and their design is based on the bending beam theory. A total of twelve strain gauges are attached on the two sides of the sensing elements (cantilever beams) to sense the strain created during the application of the load. After fabricating the sensor an experimental test is carried out and the result obtained is compared with the theoretical values. From the test it is observed that F_x is measured with 70.5%, F_y is measured with 60.9%, F_z is measured with 77.5%, M_x is measured with 63.7%, M_y is measured with 64.8% and M_z is measured with 66.1% accuracy. The results of each loads can be measured independently.

Acknowledgements

First of all I would like thank GOD for giving me time and strength to accomplish this thesis.

I would like to thank my advisor Prof. Dr.-Ing Peter Giesecke for giving me a chance to do this practical thesis work and giving me valuable and courageous advice also his support in providing full materials for this work.

My acknowledgement is also for all those who help and support me. The Mechanical Engineering Department for facilitating things to gate working materials, The Mechanical Engineering Department workshop, for suggesting ideas and supporting during manufacturing, the mechatronics laboratory technician for providing me measuring instrument.

Finally I would like to thank my friends and class mates for giving me valuable comments and suggestion.

Contents

List of Figures ……*vii*

List of Tables……*viii*

Nomenclature ……*ix*

Chapter 1 Introduction ……1

1.1 Background ……1

1.1.1 Six Component Force and Moment Sensor ……1

1.1.2 Strain Gauge Sensor and Strain Measurement……6

1.1.3 Wheatstone's Bridge……8

1.2 Objective of the thesis ……12

1.3 Methodology ……12

1.4 Organization of the thesis ……13

Chapter 2 Literature Review……14

Chapter 3 Sensor Design and Fabrication ……18

3.1 Sensor Design……18

3.1.1 Modeling the Structure of the Sensor Body ……18

3.1.2 Material of the sensor body and specification of the strain gauge ……22

3.1.3 Force/ Moment analysis ……23

3.1.4 Design of the sensing elements ……28

3.2 Sensor Fabrication ……38

3.2.1 Strain Gauge Installation and wiring ……39

3.2.2 Strain measuring instrument ……43

Chapter 4 Experimental Result and Discussion ……45

4.1 Experimental Testing……45

4.1.1 Experimental Test Setup …….....45

4.1.2 Experimental Results ……...……47

4.2 Discussing Results……...……49

4.2.1 Comparison of Strains …….....50

4.2.2 Comparison of Loads ……...53

Chapter 5 Conclusions and Future works …….……59

5.1 Conclusion …….....59

5.2 Future Work ……...…….59

Reference ……..……..…61

List of Figures

Figure 1.1 Diagram of typical wind tunnel……....4

Figure 1.2Measurement of Strain ……....6

Figure 1.3 Strain Gauge Nomenclatures……...…….7

Figure 1.4 Wheatstone bridge Circuit……....……9

Figure 1.5 Bending Beam with strain gauge……11

Figure 3.1 Structure of the sensor body……..…….…19

Figure 3.2 Skeletal of the sensor body…….....20

Figure 3.3 Cantilever Beam…….....29

Figure 3.4 Detail dimension for 2D drawing of the two half plates before bending……...…34

Figure 3.5 3D drawing of the two halve plates after bending…….....35

Figure 3.6 Connecting rods…….....36

Figure 3.7The two halves of the fabricated sensor……..38

Figure 3.8 Connecting bars with nuts……..39

Figure 3.9Foil Strain Gauge…….....40

Figure 3.10 Solder Terminal preparations……...40

Figure 3.11 P220 Sand paper……...41

Figure 3.12 Fabricated Six component force /moment sensor……43

Figure 3.13 Model P-3500 Strain Indicator…….…44

Figure 4.1 Forces and Moments Applying Position…….....46

Figure 4.2 Comparison of Actually Applied loads Vs. Measured loads ……56

List of Tables

Table 3.1 Mechanical Properties of Aluminum……..…….22

Table 3.2 Specification of the strain gauge……..23

Table 3.3 Maximum possible reactions……..…….31

Table 3.4 Summary of design data……..……33

Table 4.1 Test masses……..……46

Table 4.2 When F = 1.35 N, M = 67.5 Nmm and r = 50mm……...47

Table 4.3 When F = 1.51N, M = 75.5 Nmm and r = 50mm……47

Table 4.4 When F = 2.78N, M = 139 Nmm and r = 50mm……...…….47

Table 4.5 When F = 1.35N, M = 67.5 Nmm and r = 50mm. (Experiment I)……..……48

Table 4.6 When F = 1.51N, M = 75.5 Nmm and r = 50mm. (Experiment II)…….....48

Table 4.7 When F = 2.78N, M = 139 Nmm and r = 50mm. (Experiment III)…….....48

Table 4.8: When F = 1.35N, M = 67.5 Nmm and r = 50mm. (Experiment I)…….....49

Table 4.9: When F = 1.51N, M = 75.5 Nmm and r = 50mm. (Experiment II)……...49

Table 4.10 When F = 2.78N, M = 139 Nmm and r = 50mm. (Experiment III)……..…49

Table 4.11 Comparison of theoretical and experimental strain results……50

Table 4.12 Comparing Actual and measured Forces from the first experiment……..53

Table 4.13 Comparing Actual and measured Forces from the second experiment…….54

Table 4.14 Comparing Actual and measured Forces from the third experiment……..…54

List of Symbols

CB - cantilever beam

E- Modules of elasticity

E- Input voltage

e- out put voltage

F- Force vector

F_x, F_y, F_z –applied forces

F_1, F_2, F_3, F_4, F_5, F_6 –reaction forces

GF- gauge Factor

H, *h*- height

I- moment of inertia

L, *l* - Length

ΔL- length change

Mx, My, Mz – applied moments

R-resistance

ΔR-resistance change

S – Section modules

T, t - thickness

W, w -width

ε –strain

μ- Micro

σ- Stress

σ_b- bending stress

CHAPTER ONE

INTRODUCTION

1.1 Background

Accurate Measurement of multi component forces and moments applied on an object is especial interest in today's technological development. The need for measuring these forces/moments is to control (increase or decrease) the force/moment exerted on it in different directions and to protect machine components from over loading or damage. It is widely applied especially in industries and research areas. For example the trend of industrial automation increasingly requires the use of robotic manipulators to serve works such as installation, welding, grinding and object gripping/moving.

1.1.1 Six Component Force and Moment Sensor

A six-component force sensor is a device which functions simultaneously to measure six forces, three orthogonal forces and three orthogonal moments, and is used for wind-tunnel balances, thrust stand testing of rocket engines, automobiles, shipbuilding, and particularly quite common for adaptive real-time control purpose of machines such as robotic systems.

The six component measuring device basically measures all measurable physical quantities that may cause a mechanical deformation of a solid body, i.e. in particular the force F, the mass m, the torque T, the bending moment M, the hydraulic pressure p and the acceleration a.
A special position is a measuring task that requires the simultaneous detection of several forces and

moments. The first and most demanding application of such measurements goes back to the beginning of last century, and even here back to the beginnings of systematic aircraft development. At that time the aerodynamics of a largely unexplored area, and correspondingly great was the interest in experimental data. The most important and meaningful investigation it turned out on the measurement of an aircraft model in wind tunnel aerodynamic forces and moments acting, and so we are already at the six-component measurement. The actual measuring task is simple: to be measured as a function of the flow velocity perpendicular to each force sizes resistance, lift and side force and the associated moments roll, yaw and pitch moment.

The measuring device used has gone through over the course of the century, three developmental stages had passed and the last of which opened the door for a wide field has very different bearing applications. The earliest multi-component type transducer was composed from mechanically-isolated measurement channels simple mechanism particularly well suited for demonstrating the decoupling mechanisms. This so-called wind tunnel scale originally consisted of a very complex mechanical device for mechanical decoupling of the six components, each with a sliding weight scales for weighing the respective component. The special design of this measuring device required a large amount of space, so it was arranged outside the duct and connected to the flight model by wires or stems. The weighing operation lasted for up to several seconds and did not allow dynamic measurements. Therefore, the first improvement was the replacement of the sliding weight scales with strain gauge load cells, which were about from the seventies with sufficient accuracy. The complex mechanical decoupling of the six components required but still a lot of space with appropriate maintenance and adjustment to maintain measurement accuracy.
The end of the seventies made second improvement in the mechanical decoupling caused typical mechatronic approach by a calculation method. The really decisive progress achieved but only with

the last step, the space requirement reduction of approximately up to 50 m³ in volume. This radical reduction in volume was both in the aircraft and the sensor industries. The developers took advantage of the low space requirement, because they could now integrate directly from one part of the existing six-component sensor in the aircraft model, for example, this reduced quite considerably influences the flow and improved due to the high stiffness of the dynamic behavior.

a. Wind Tunnel

A wind tunnel is a research facility in which working section model tests are conducted. The working section of a wind tunnel is a critical part through which air is blown or sucked to the required velocity or Mach number to study the effects of aerodynamics resulting from the flow around scale models or other objects mounted in the test section.

Wind tunnels can be classified into three types according to flow speed in the test section (Donovan and Goddard, 1961 [8]): low speed (working section Mach numbers less than 0.5), high speed (working section Mach numbers between 0.5 and 5), and hypersonic (working section Mach numbers greater than 5). They can also be divided into continuous, intermittent, and impulse wind tunnels according to their running time. Wind tunnels mainly consist of a body, driving system, and a control and measurement system, which can vary in different wind tunnels. The body contains test sections with uniform flow for tests and other sections for improving the flow quality and for reducing the energy consumption. The driving system includes the systems for driving flow and for controlling the model attitude. The control and measurement system comprises the modules for control and measurement of flow field and model attitude as well as the module for the measurement of some physical quantities such as pressure and temperature.

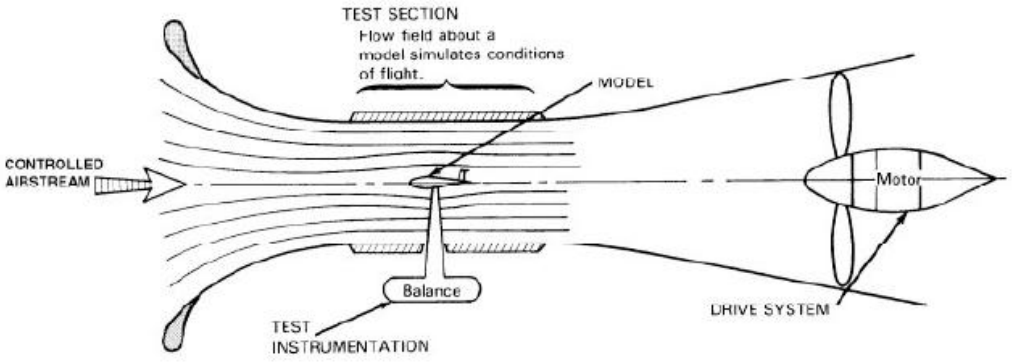

Figure 1.1 Diagram of typical wind tunnel

One of the most important functions of wind tunnels is to provide estimates of the aerodynamic loads acting on bodies moving through air. These estimates must be measured somehow. The first such measurements were obtained using actual balances. Since then, aerodynamic load measurement

b. Wind Tunnel Balance

Measurement of steady and fluctuating forces acting on a body in a flow is one of the main tasks in wind tunnel experiments. The key measurement system in a wind tunnel is the Multi-component force and moment measurement instrumentation. More than 70% [7] of the tests in a wind tunnel require some kind of force measurements.

A six component Force and Moment Balances is a device used to measures aerodynamic loads a model experience during a wind tunnel test. It enables to measure the three orthogonal forces i.e. Drag Force, Side Force and Normal Force and the three orthogonal moments i.e. Rolling Moment, Yawing Moment and Pitching Moment simultaneously.

There are several types of wind tunnel balances. The most important are:

External balances: They are placed outside the model, inside or outside the wind tunnel chamber test section, but they always introduce some interference in the wind flow. However the possibility to change test models with almost no effort provides a high flexibility to the wind tunnel facility. There are several degrees of complexity for these balances, depending mainly on the number of measurement channels, which can vary between 1 and 6.

Internal balances*:* They are placed inside the model, thus no interferences are introduced in the wind flow by the balance components, but a mechanical support for the model is always needed to maintain it in the test chamber and change the model orientation if desired. The complexity of the test model is comparable or higher than the models for scanivalve systems, as the balance has to be installed inside. Thus this option does not provide flexibility in testing different models. The number of measured components can also vary between 1 and 6.

Rotary balances*:* Used for propellers, helicopter blades and other rotating models.

Six Component Balances are also divided into [8] mechanical balances, strain gauge balances, piezoelectric balances, and magnetic suspension balances according to the measurement principle.

A mechanical balance is a device to measure the aerodynamic force and moment by its mechanical force equilibrium elements or force transducers, after decomposing the force and the moment of the model into its mechanic components.

A strain gauge balance measures force and moment using a Wheatstone bridge that captures the electric effect of the strain gauge deformation when the balance is loaded. At present, strain gauge balances are the most widely employed for force and moment measurements in wind tunnels. Along with the sting-type strain gauge balance and the box-type strain gauge balance, there are a number of special strain gauge balances to meet the requirements of special measurements, for example, hinge

moment balances, dynamic derivate balances, jet balances, Magnus balances, rotating balances, rotating wing balances, parachute balances, high temperature balances, low-temperature balances, friction stress balances, mini-rolling moment balances, micro-range balances, stress wave balances, and so on.

1.1.2 Strain Measurement and Strain Gauge Sensor

a. Strain

Strain is a measure of the deformation of a body when subject to an applied force. Specifically, strain (ε) is the fractional change in length of a body when subject to a force along its length. That is:

$$\varepsilon = \frac{\Delta L}{L} \quad (1.1)$$

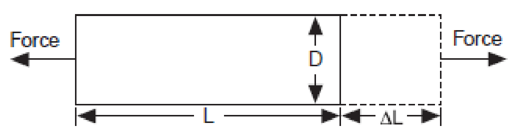

Figure 1.2 Measurement of Strain

Note that strain can be either positive (tensile), or negative (compressive). Further, the magnitude of a strain measurement is typically very small and is often expressed as a whole number multiple of 10^{-6}, or micro strain (μ ε). In most cases, strain measurements are rarely encountered larger than a few milli strain (ε x 10^{-3}), or about 3000μ ε, except for high-elongation applications.

b. Strain Gauges

Strain gauges are devices that change resistance slightly in response to an applied strain. These devices typically consist of a very fine foil grid (or wire grid) that is bonded to a surface in the direction of the applied force. The cross-sectional area of this device is minimized to reduce the negative effect of the shear or Poisson's Strain. These devices are commonly referred to as bonded-metallic or bonded-resistance strain gauges. The foil grid is bonded to a thin backing material or carrier which is directly attached to the test body. As a result, the strain experienced by the test body is transferred directly to the foil grid of the strain gauge, which responds with a linear change (or nearly linear change) in electrical resistance. As you can surmise, properly mounting a strain gauge is critical to its performance in ensuring that the applied strain of a material is accurately transferred through the adhesive and backing material, to the foil itself.

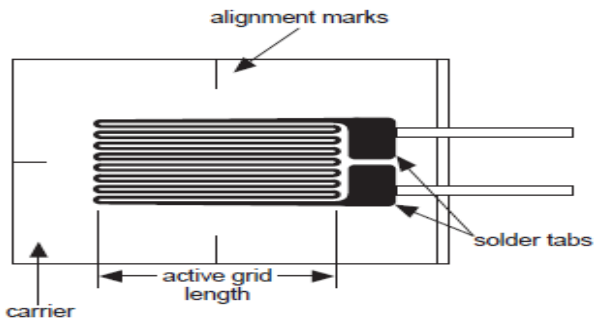

Figure 1.3 Strain Gauge Nomenclatures

Strain gauges are widely employed in sensors that detect and measure force and force-related parameters, such as torque, acceleration, pressure, and vibration. The strain gauge is the building block for strain sensors that often employ multiple strain gauges in their construction.

A strain gauge will undergo a small mechanical deformation with an applied force that results in a small change in gauge resistance proportional to the applied force.

Because this change in resistance with applied force is so small, strain gauges are commonly wired using a Wheatstone bridge. The resultant output voltage of the bridge is directly related to any imbalance between resistances in each leg of the bridge and the bridge excitation voltage. The output of the bridge is normally specified in terms of millivolts of output voltage per volt of applied excitation (mV/V), and this is usually referred to as its rated output or sensitivity. The actual maximum or full-scale output of a strain gauge bridge at its full-rated load is the product of a bridge's sensitivity (mV/V) and the applied excitation voltage. This is referred to as the output span under full rated load.

The relationship between the resultant fractional changes of gauge resistance (ΔR) to the applied strain (fractional change of length) is called the Gauge Factor (GF), or sensitivity to strain. Specifically, the Gauge Factor is the ratio of the fractional change in resistance to the strain:

$$GF = \frac{(\Delta R/R)}{(\Delta L/L)} = \frac{(\Delta R/R)}{\varepsilon} \quad \text{.....} \quad (1.2)$$

The Gauge Factor for metallic strain gauges is typically around 2.0. However, it is important to note that this ratio will vary slightly in most applications and a method of accounting for the effective Gauge Factor of a strain measurement system must be provided.

1.1.3 Wheatstone's Bridge

The Wheatstone bridge is a circuit able to detect small changes in resistance and convert it to output voltage when an input voltage is given to it. It is comprised of four resistive arms arranged in the configuration of a diamond as shown below. An excitation voltage is applied across the diamond (or

bridge input), and a resultant output voltage can be measured across the other two vertices of the diamond as shown.

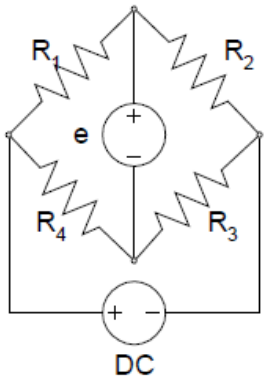

Figure 1.4 Wheatstone bridge Circuit

The output voltage (e) can be written as the difference between two ballast circuits as:

$$e = [\frac{R_2}{R_1+R_2} - \frac{R_3}{R_3+R_4}]E \quad \text{..... (1.3)}$$

Clearly, an initial steady state voltage exists unless the numerator above is zero. Such a configuration with zero output voltage is termed a "Balanced Bridge" and is provided when:

$$R2\ R4 = R1\ R3 \quad \text{..... (1.4)}$$

This relationship is not of direct concern here but it is interesting to note that if any three of the four resistances are known, the fourth can be determined by ratioing the values obtained at balance. For the present, however, we are concerned with the output produced by small changes in the resistance of the bridge arms. If we consider infinitesimal changes in each resistor then

$$R_i \Rightarrow R_i + dR_i \quad \text{..... (1.5)}$$

and we can compute the differential change in the output voltage, e, as:

$$de = \frac{\partial e}{\partial R_1} dR_1 + \frac{\partial e}{\partial R_2} dR_2 + \frac{\partial e}{\partial R_3} dR_3 + \frac{\partial e}{\partial R_4} dR_4 \quad \text{..... (1.6)}$$

Or $$de = \left[\frac{R_1R_2}{(R_1+R_2)^2}\left(\frac{dR_1}{R_1} - \frac{dR_2}{R_2}\right) + \frac{R_3R_4}{(R_3+R_4)^2}\left(\frac{dR_3}{R_3} - \frac{dR_4}{R_4}\right)\right] E \quad \text{..... (1.7)}$$

If the bridge is balanced so that:

$$R = R1 = R2 = R3 = R4 \quad \text{..... (1.8)}$$

then using this in the above equation for *de* yields:

$$de = \frac{1}{4}\left[\frac{dR_1}{R_1} - \frac{dR_2}{R_2} + \frac{dR_3}{R_3} - \frac{dR_4}{R_4}\right] E \quad \text{.....(1.9)}$$

We can use Eq. 1.2 to express *de* in terms of the strains as:

$$de = \frac{GF}{4}[\varepsilon_1 - \varepsilon_2 + \varepsilon_3 - \varepsilon_4] E \quad \text{..... (1.10)}$$

The basic equation relating the Wheatstone bridge output voltage to strain in gages placed in each arm can be written as:

$$e = \frac{GF}{4}[\varepsilon_1 - \varepsilon_2 + \varepsilon_3 - \varepsilon_4] E \quad \text{..... (1.11)}$$

There are a number of variations in the bridge wiring and the configuration of active and dummy gages that can provide suitable performance for different applications.

Quarter Bridge: when only one arm is active and the other three rams are dummy.

Half Bridge: when two arms are active and the other two arms are dummy.

Full Bridge: when all four arms are active

Half Bridge Circuit:

The most useful application of this circuit is in the measure of bending strain in a thin plate or beam.

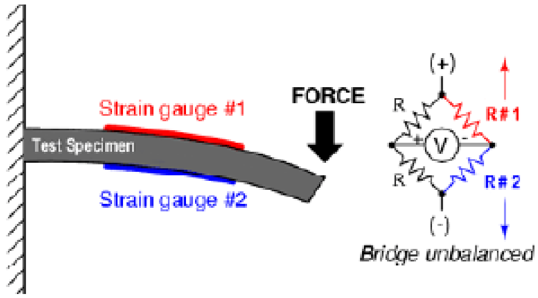

Figure 1.5 Bending Beam with strain gauge

In this case the two gages are mounted opposite each other on opposite (top/bottom) surfaces so that a compressive strain ($-\varepsilon_b$) is introduced in one and an equal tensile strain (ε_b) in the other. Then:

$$e = \frac{GF}{4}(\varepsilon_b - (-\varepsilon_b))\, E = \frac{GF}{2}\varepsilon_b\, E \quad \ldots\ldots\ldots\ldots\ldots\ldots\ldots\ldots\ldots\ldots\ldots\ldots\ldots\ldots\ldots \quad (1.12)$$

Statement of the problem

Six component sensors are widely used in determining aerodynamic loads applied on a model in wind tunnel or in controlling robotic loads applied by the robot and any similar applications. In order to analyze these loads especially in wind tunnel different types of multicomponent sensors can be used. Most of the six component sensors used in wind tunnel can be categorized in to two main types according to their position in the wind tunnel. These are internal and external types. The internal type sensor is inserted inside the model while the external one is situated outside the model and the wind tunnel.

In designing these sensors their shape, structure, measuring accuracy and cost are the main determining factors. Most of the internal type sensors are small sized and monolithic cross bar structures. Due to this it requires high level of engineering to manufacture them. This in turn increases their manufacturing cost. On the other hand the external type sensors can be designed with large size, relative to the internal one, with different structure. There are different types of

commercial external balances in use today. But most of them have complicated structure and they are costy. There are also several types of external sensors in use in different research centers with continuous improvement.

The cost of the sensors is mostly related to the complexity of the structure used. This can be minimized by designing a simple structure which can be manufactured easily. So it is necessary to design simple structure, low cost sensor with the required accuracy level.

In this study a new type six component strain gauge sensor, which can measure six component loads (three forces and three moments), is designed and manufactured. All the six component loads can be measured simultaneously.

1.2 Objective of the Thesis

Main objective

The main objective of the study is to design low cost and simple structure sensor which can measure six component force and moment simultaneously in wind tunnel and robotic system.

Specific Objectives

The specific objectives of the study are:

- ✓ Developing simple structure sensor body to achieve minimum cost
- ✓ Designing for the developed sensor structure and identifying the location of attachments of the strain gauges
- ✓ Manufacturing and testing sensor as per the design condition

1.3 Methodology

To achieve the desired objectives the following methods are employed.

I. **Literature Review:** Related literatures are consulted from different sources like books, journal articles, proceedings of international conferences and different catalogues

II. **Design and manufacturing:** The sensor body structure is developed, designed and manufactured

III. **Experimental testing and discussion of results:** The manufactured sensor is tested and the result is discussed by comparing with the theoretical values

IV. **Conclusion:** conclusions are given based on the experimental results

1.4 Structure of the Thesis

Chapter one covers introduction part. It introduces about six component measurement and its application especially in wind tunnel. It also gives emphasis on strain measurement system, Wheatstone bridge circuit and its application in bending beam analysis. Chapter two provides review of literature from different sources. Chapter three is about the design and Fabrication process. It provides the method for determining the size of the sensor and specifies the location of attachment of strain gauges as well as the fabrication and installation of strain gauge. The fourth chapter is about testing of the sensor and discussion of the test results. Finally the last chapter draws a conclusion based on the result obtained during the test.

CHAPTER TWO

LITERATURE REVIEW

The growing demand on measuring technology has led a decisive change in the construction of variety of multi component sensors for different application. A six-component force sensor is a unit which functions to simultaneously measure six forces, three orthogonal forces and three orthogonal moments, and is used for wind-tunnel balances, thrust stand testing of rocket engines, automobiles, shipbuilding, and particularly quite common for adaptive real-time control purpose of machines such as robotic systems [9]. The main purpose of this study is to design and manufacture a new six component force and moment sensor which can measure three forces (drag, lift and side forces) and three moments (roll, pitch and yaw moments) simultaneously. In this study Previous works that had been done up to recent time is consulted from related literatures.

Variety of multi component sensors has been developed in the past. A Maltese crossbar seems to be the earliest elastic structure developed [4] for a six-component force sensor. It responds to some force components with relatively higher stiffness than to others, ensuring a poor measurement isotropy. In addition to this particular structural deficiency, the measurements based on this bar present a high degree of coupling. For improvements on these deficiencies, it requires that more strain gauges be imposed in the sensing bridges. This inevitably introduces error sources.

Chao and Chen [11] modified the Maltese crossbar by using ball bearings on the outer sides of the four spokes to allow sliding and rotating at the rims. Although such an idea is quite novel and

attractive, it may introduce behavior deficiencies such as nonlinearity, non-repeatability, and hysteresis.

Kim [1] designed and fabricated a small capacity 6-axis force/moment plate beam sensor to measure forces Fx , Fy and Fz, and moments Mx , My and Mz, simultaneously in industry. He newly modeled the structure of the sensing element and proposed a method for calibrating the sensor. He also designed [2] a small six-axis force/moment sensor which can be mounted on robot's fingers.

Farhad A, et al [10] designed a new one axis torque sensor for robot joints. He achieved the conflicting requirements of high stiffness for all six force and torque components, high sensitivity for the one driving torque of interest, and yet very low sensitivity for the other five force/torque components.

Yabuki [14] developed a six-component force/moment sensor using parallel plates for controlling robots. Hatamura *et al* [15] developed a six-component force/moment sensor using radial plates for measuring forces and moments in industry.

Makoto Kaneko [16][17] proposed an interesting design of twin head multi axis force sensor based on the principle of pressure pick-up device. The new six axis force sensor is composed of two three-axis force sensors and connector. He described the theoretical basis for the operation of this type of sensor and provided the characteristics matrix connecting the load and sensor output vectors.

Chul-Goo Kang [12] proposed a method to improve the performance of a six axis Force-torque sensor with double-hole structure. He distinguished error sources in to two categories structural error due to inaccuracies of sensor body, and noise signal from the sensed information. He claimed that the structural error can be improved by using double-hole structure and signal to noise ratio (S/N) can also be improved through signal conditioning.

Recently multi-component sensors were also used in new fields. Shengmi Wang [21] designed a six-axis endoscopic force/torque sensor using strain gauge for use in minimal invasive surgery. In designing micro-robots six-component sensors play a vital role [22]-[23].

In wind tunnel test six component sensors have an important application to determine drag, lift and side forces and roll, pitch, and yaw moments applied on a full or scale model. These sensors may be internal or external type. Most of the six component sensors are internal type. Lincoln P. et. al [5] developed five-component strain gauge internal balance using the same principle with a two component balance developed earlier at DSTO to measure flow induced loads on models in the DSTO water tunnel.

Timm Preusser and Lubomir Polansky [13] developed six component external balance. They developed a new type of strain gauge balance which combines the advantageous features of computer separation with the conceptional advantages of both platform and pyramidal type balances. This allows for a significant reduction of load cells required, for calibration of different datum heights within the test section, and for considerable improvement of measurement accuracy of roll, pitch and yaw moments. The basic metrological features of multi-component strain gauge sensors are determined to a great extent by the shapes and sizes of elastic elements on which the strain gauges are bonded [18]-[20].

Marin Sandu et.al [6] developed a six component force/moment sensor which can be used either as internal or as external balance in the aerodynamic testing of air craft models in wind tunnel. But the structure he modeled was complicated and used more than 20 strain gauges which maximize the manufacturing and total cost of the balance.

This study presents the design of a new external six component force/moment sensor. The sensing principle is based on the measurement of the deformation of the cantilever beam using strain gauge

attached on it. The design and fabrication process of the sensor is briefly described in the next chapters.

CHAPTER THREE

Sensor Design and Fabrication

3.1 Sensor Design

3.1.1 Modeling The Structure of the Sensor Body

Forces and moments applied to the sensor are evaluated through the measurement of strains on the sensor body. The sensor body is a structural system with especially designed shape. Evaluation of forces and moments is based on the principle of the deformation of a cantilever beam, which has strain gauges attached on it, in its elastic range.

The CAD model of the six component sensor structure is shown in figure 3.1 below. It is composed of two 90^o bend plates $\mathbf{P}_1$ and $\mathbf{P}_2$ (left and right halves) which have inbuilt cantilever beams CB_1, CB_2, CB_3, CB_4, CB_5 and CB_6; force and moment transmitting bars B_1, B_2, B_3, B_4, B_5 and B_6; and nuts to securely fix force and moment transmitting bars with the two 90^o bend plates. All these components together form a rectangular box type structure whose over all dimensions are Length (**L**), Width (**W**), Height (**H**) and Thickness (**T**). The forces (F_x, F_y and F_z) and moments (M_x, M_y and M_z) are measured from the strain signal obtained from the deflection of the surface of cantilever beams. The sizes of the cantilever beams CB_1-CB_6 are Length (l_i), width (b_i) and thickness (t_i) where i = 1, 6. Distances *a*, *b*, *c*, *d*, *f*, *g* and *h* are the distance between the reactions and the load application point (reference coordinate OXYZ).

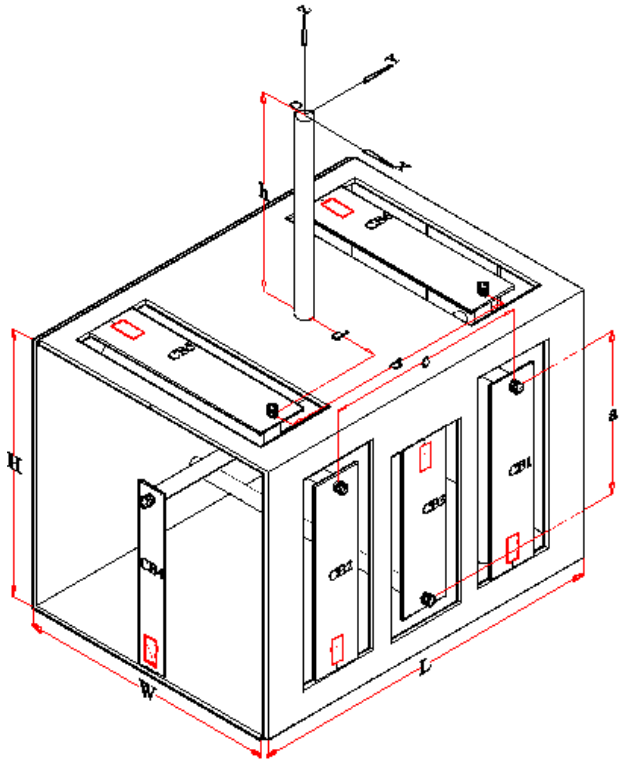

Figure 3.1 Structure of the sensor body

When a force vector **F**= (F_x, F_y, F_z, M_x, M_y, M_z) is applied at the coordinate OXYZ, it is transmitted to the cantilever beams through the connecting bars. The reaction of the connecting bars to the applied loads creates bending stress on the cantilever beams. The bending stress in turn creates strain on the surface of the cantilever beams.

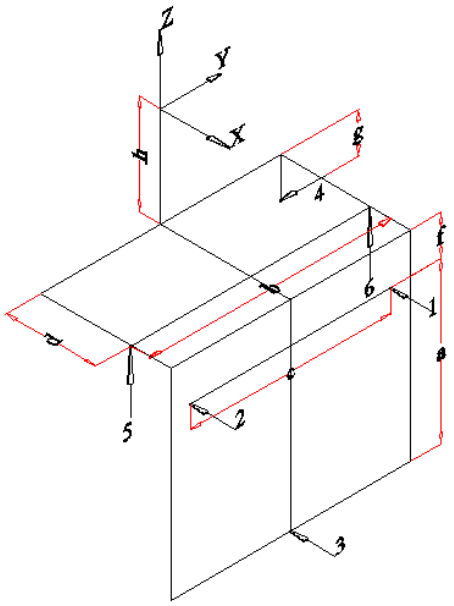

Figure 3.2 Skeletal of the sensor body

The equilibrium equation when the load vector **F**= (F_x, F_y, F_z, M_x, M_y, M_z) applied at the coordinate OXYZ is obtained as follows.

$$Fx = F1 + F2 + F3 \quad \text{.....} \quad (3.1a)$$

$$Fy = F4 \quad \text{.....} \quad (3.1b)$$

$$Fz = -F5 - F6 \quad \text{.....} \quad (3.1c)$$

$$Mx = (h + g)F4 + \left(\frac{b}{2}\right)F5 - (b/2)F6 \quad \text{.....} \quad (3.1d)$$

$$My = -(h + f)F1 - (h + f)F2 - (a + f + h)F3 + dF5 + dF6 \quad \text{.....} \quad (3.1e)$$

$$Mz = -\left(\frac{c}{2}\right)F1 + \left(\frac{c}{2}\right)F2 \quad \text{.....} \quad (3.1f)$$

In matrix form it can be rewritten as

$$\begin{Bmatrix} Fx \\ Fy \\ Fz \\ Mx \\ My \\ Mz \end{Bmatrix} = \begin{bmatrix} 1 & 1 & 1 & 0 & 0 & 0 \\ 0 & 0 & 0 & 1 & 0 & 0 \\ 0 & 0 & 0 & 0 & -1 & -1 \\ 0 & 0 & 0 & (h+g) & \left(\frac{b}{2}\right) & -(b/2) \\ -h & -h & -(a+f+h) & 0 & d & d \\ -\left(\frac{c}{2}\right) & \left(\frac{c}{2}\right) & 0 & 0 & 0 & 0 \end{bmatrix} . \begin{bmatrix} F_1 \\ F_2 \\ F_3 \\ F_4 \\ F_5 \\ F_6 \end{bmatrix} \quad \ldots\ldots\ldots\ldots (3.2)$$

The unknown reaction forces can be obtained from the inverse decoupled matrix of the above equilibrium equation using mat lab.

Mat lab program

```
>> syms a b c d f g h
>> A=[1 1 1 0 0 0;0 0 0 1 0 0;0 0 0 0 -1 -1;0 0 0 (h+g) b/2 -b/2;-h -h -(a+f+h) 0 d d;-c/2 c/2 0 0 0 0]
 A =
 [     1,     1,     1,     0,     0,     0]
 [     0,     0,     0,     1,     0,     0]
 [     0,     0,     0,     0,    -1,    -1]
 [     0,     0,     0,   h+g, 1/2*b, -1/2*b]
 [    -h,    -h, -a-f-h,     0,     d,     d]
 [-1/2*c, 1/2*c,     0,     0,     0,     0]
  >> B=inv(A)
 B =
 [ 1/2*(a+f+h)/(a+f),          0,     1/2*d/(a+f),          0,     1/2/(a+f),          -1/c]
 [ 1/2*(a+f+h)/(a+f),          0,     1/2*d/(a+f),          0,     1/2/(a+f),           1/c]
 [       -h/(a+f),             0,       -d/(a+f),           0,       -1/(a+f),            0]
 [              0,             1,              0,           0,              0,            0]
 [              0,      -(h+g)/b,           -1/2,         1/b,              0,            0]
 [              0,       (h+g)/b,           -1/2,        -1/b,              0,            0]
```

Thus the unknown reactions are

$$\begin{Bmatrix} F_1 \\ F_2 \\ F_3 \\ F_4 \\ F_5 \\ F_6 \end{Bmatrix} = \begin{bmatrix} \frac{(a+f+h)}{2(a+f)} & 0 & \frac{d}{2(a+f)} & 0 & \frac{1}{2(a+f)} & \frac{-1}{c} \\ \frac{(a+f+h)}{2(a+f)} & 0 & \frac{d}{2(a+f)} & 0 & \frac{1}{2(a+f)} & \frac{1}{c} \\ \frac{-h}{(a+f)} & 0 & \frac{-d}{(a+f)} & 0 & \frac{-1}{(a+f)} & 0 \\ 0 & 1 & 0 & 0 & 0 & 0 \\ 0 & \frac{-(h+g)}{b} & -0.5 & \frac{1}{b} & 0 & 0 \\ 0 & \frac{(h+g)}{b} & -0.5 & \frac{-1}{b} & 0 & 0 \end{bmatrix} \cdot \begin{bmatrix} Fx \\ Fy \\ Fz \\ Mx \\ My \\ Mz \end{bmatrix} \quad \ldots\ldots\ldots\ldots (3.3)$$

3.1.2 Material of the sensor body and specification of the strain gauge

The material of the sensor body is chosen to be Aluminum plate with 1.5 mm thickness. Aluminum is preferred because it has low density compared with steel plate. This reduces initial strain due to self-weight of the upper half of the plate without the application of the load. Based on this the selected material has the following characteristics.

Table 3.1 Mechanical Properties of Aluminum

Modulus of Elasticity (E)	69 GPa
Density	2.7 g/cm^3
Tensile strength	324MPa
Yield strength	169MPa
Poison's ratio	0.33

Table 3.2 Specification of the strain gauge

<table>
<tr><td colspan="5">Strain Gauge Specification</td></tr>
<tr><td>Strain gauge construction</td><td colspan="4">Foil SG complete with embedded measuring grid</td></tr>
<tr><td>Measuring grid material</td><td colspan="4">Constantan foil</td></tr>
<tr><td>Carrier material</td><td colspan="4">Polyimide</td></tr>
<tr><td>Cover material</td><td colspan="4">Polyimide</td></tr>
<tr><td>Nominal Resistance</td><td colspan="4">350 Ω</td></tr>
<tr><td>Gage Factor (GF)</td><td colspan="4">App. 2</td></tr>
<tr><td>Operating temperature range</td><td colspan="4">-200°c … + 180°c</td></tr>
<tr><td>Bonding material that can be used (in cold curing adhesive)</td><td colspan="4">Z70 Adhesive</td></tr>
<tr><td rowspan="3"> 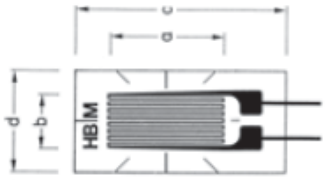 </td><td colspan="2">Measuring Grid</td><td colspan="2">Measuring Grid Carrier</td></tr>
<tr><td>A</td><td>B</td><td>C</td><td>D</td></tr>
<tr><td>6</td><td>2.8</td><td>13</td><td>6</td></tr>
</table>

3.1.3 Force/Moment Analysis

The forces/moments applied on the sensor can be analyzed in terms of the strains developed at the location of attachment of the strain gauges. This strain is due to the reaction force created at the free end of the cantilever beam when a force or moment is applied at OXYZ coordinate point. Therefore,

it is necessary to know the reaction when a single force F_i or moment M_i is applied and at the end the aggregate sum when all forces and moments are applied.

a) When a force F_x is applied

When a single force F_x is applied at the coordinate point OXYZ, the cantilever beams CB_1, CB_2 and CB_3 reacts a force F_1, F_2 and F_3 respectively through the rigid connecting rods. The cantilever beams CB_4, CB_5 and CB_6 have no response or reaction for F_x force. Therefore

$$F_4 = F_5 = F_6 = 0$$

Then reaction forces are obtained from eqn. (3.3) by substituting only F_x.

$$\begin{Bmatrix} F_1 \\ F_2 \\ F_3 \\ F_4 \\ F_5 \\ F_6 \end{Bmatrix} = \begin{bmatrix} \frac{(a+f+h)}{2(a+f)} & 0 & \frac{d}{2(a+f)} & 0 & \frac{1}{2(a+f)} & \frac{-1}{c} \\ \frac{(a+f+h)}{2(a+f)} & 0 & \frac{d}{2(a+f)} & 0 & \frac{1}{2(a+f)} & \frac{1}{c} \\ \frac{-h}{(a+f)} & 0 & \frac{-d}{(a+f)} & 0 & \frac{-1}{(a+f)} & 0 \\ 0 & 1 & 0 & 0 & 0 & 0 \\ 0 & \frac{-(h+g)}{b} & -0.5 & \frac{1}{b} & 0 & 0 \\ 0 & \frac{(h+g)}{b} & -0.5 & \frac{-1}{b} & 0 & 0 \end{bmatrix} . \begin{bmatrix} Fx \\ 0 \\ 0 \\ 0 \\ 0 \\ 0 \end{bmatrix} \quad \ldots\ldots\ldots\ldots (3.4)$$

$$F_1 = \frac{(a+f+h)}{2(a+f)} F_x$$

$$F_2 = \frac{(a+f+h)}{2(a+f)} F_x$$

$$F_3 = \frac{-h}{(a+f)} F_x$$

b) When a force F_y is applied

When a single force F_y is applied at the coordinate point OXYZ, cantilever beams CB_4, CB_5 and CB_6 reacts forces F_4, F_5 and F_6 through the rigid connecting rods. The cantilever beams CB_1, CB_2, and CB_3 have no response or reaction for F_y force. Therefore

$$F_1 = F_2 = F_3 = 0$$

Then the reaction force is obtained from eqn. (3.3) by substituting only F_y.

$$\begin{Bmatrix} F_1 \\ F_2 \\ F_3 \\ F_4 \\ F_5 \\ F_6 \end{Bmatrix} = \begin{bmatrix} \frac{(a+f+h)}{2(a+f)} & 0 & \frac{d}{2(a+f)} & 0 & \frac{1}{2(a+f)} & \frac{-1}{c} \\ \frac{(a+f+h)}{2(a+f)} & 0 & \frac{d}{2(a+f)} & 0 & \frac{1}{2(a+f)} & \frac{1}{c} \\ \frac{-h}{(a+f)} & 0 & \frac{-d}{(a+f)} & 0 & \frac{-1}{(a+f)} & 0 \\ 0 & 1 & 0 & 0 & 0 & 0 \\ 0 & \frac{-(h+g)}{b} & -0.5 & \frac{1}{b} & 0 & 0 \\ 0 & \frac{(h+g)}{b} & -0.5 & \frac{-1}{b} & 0 & 0 \end{bmatrix} . \begin{bmatrix} 0 \\ Fy \\ 0 \\ 0 \\ 0 \\ 0 \end{bmatrix} \quad \ldots\ldots\ldots\ldots (3.5)$$

$$F_4 = F_y$$

$$F_5 = \frac{-(h+g)}{b} F_y$$

$$F_6 = \frac{(h+g)}{b} F_y$$

c) When a force F_z is applied

When a single force F_z is applied at the coordinate point OXYZ, the cantilever beams CB_1, CB_2, CB_3, CB_5 and CB_6 react forces F_1, F_2, F_3, F_5 and F_6 through the rigid connecting rods. The cantilever beam CB_4 has no response or reaction for F_z force. Therefore

$$F_4 = 0$$

Then reaction forces are obtained from eqn. (3.3) by substituting only F_z.

$$\begin{Bmatrix} F_1 \\ F_2 \\ F_3 \\ F_4 \\ F_5 \\ F_6 \end{Bmatrix} = \begin{bmatrix} \frac{(a+f+h)}{2(a+f)} & 0 & \frac{d}{2(a+f)} & 0 & \frac{1}{2(a+f)} & \frac{-1}{c} \\ \frac{(a+f+h)}{2(a+f)} & 0 & \frac{d}{2(a+f)} & 0 & \frac{1}{2(a+f)} & \frac{1}{c} \\ \frac{-h}{(a+f)} & 0 & \frac{-d}{(a+f)} & 0 & \frac{-1}{(a+f)} & 0 \\ 0 & 1 & 0 & 0 & 0 & 0 \\ 0 & \frac{-(h+g)}{b} & -0.5 & \frac{1}{b} & 0 & 0 \\ 0 & \frac{(h+g)}{b} & -0.5 & \frac{-1}{b} & 0 & 0 \end{bmatrix} . \begin{bmatrix} 0 \\ 0 \\ Fz \\ 0 \\ 0 \\ 0 \end{bmatrix} \quad \ldots\ldots\ldots\ldots (3.6)$$

$$F_1 = \frac{d}{2(a+f)} F_z$$

$$F_2 = \frac{d}{2(a+f)} F_z$$

$$F_3 = \frac{-d}{(a+f)} F_z$$

$$F_5 = \frac{-1}{2} F_z$$

$$F_6 = \frac{-1}{2} F_z$$

d) When a moment M_x is applied

The sensing elements for the Mx sensor are the cantilever beams CB_5 and CB_6. When a moment M_x is applied, the cantilever beams CB_5 and CB_6 react forces F_5 and F_6 through the rigid connecting rods. The other beams have no reaction. Therefore

$$F_1 = F_2 = F_3 = F_4 = 0$$

Then reaction forces are obtained from eqn. (3.3) by substituting only M_z.

$$\begin{Bmatrix} F_1 \\ F_2 \\ F_3 \\ F_4 \\ F_5 \\ F_6 \end{Bmatrix} = \begin{bmatrix} \frac{(a+f+h)}{2(a+f)} & 0 & \frac{d}{2(a+f)} & 0 & \frac{1}{2(a+f)} & \frac{-1}{c} \\ \frac{(a+f+h)}{2(a+f)} & 0 & \frac{d}{2(a+f)} & 0 & \frac{1}{2(a+f)} & \frac{1}{c} \\ \frac{-h}{(a+f)} & 0 & \frac{-d}{(a+f)} & 0 & \frac{-1}{(a+f)} & 0 \\ 0 & 1 & 0 & 0 & 0 & 0 \\ 0 & \frac{-(h+g)}{b} & -0.5 & \frac{1}{b} & 0 & 0 \\ 0 & \frac{(h+g)}{b} & -0.5 & \frac{-1}{b} & 0 & 0 \end{bmatrix} \cdot \begin{bmatrix} 0 \\ 0 \\ 0 \\ Mx \\ 0 \\ 0 \end{bmatrix} \quad \ldots\ldots\ldots\ldots (3.7)$$

$$F_5 = \frac{1}{b} M_x$$

$$F_6 = \frac{(-1)}{b} M_x$$

e) When a moment M_y is applied

The sensing elements for the M_y sensor are the cantilever beams CB_1, CB_2, and CB_3. When the moment M_y is applied, the cantilever beams CB_1, CB_2, and CB_3, react a force F_1, F_2, and F_3 respectively through the rigid connecting rods. CB_4, CB_5 and CB_6 have no reaction. Therefore

$$F_4 = F_5 = F_6 = 0$$

Then reaction forces are obtained from eqn. (3.3) by substituting only M_y.

$$\begin{Bmatrix} F_1 \\ F_2 \\ F_3 \\ F_4 \\ F_5 \\ F_6 \end{Bmatrix} = \begin{bmatrix} \frac{(a+f+h)}{2(a+f)} & 0 & \frac{d}{2(a+f)} & 0 & \frac{1}{2(a+f)} & \frac{-1}{c} \\ \frac{(a+f+h)}{2(a+f)} & 0 & \frac{d}{2(a+f)} & 0 & \frac{1}{2(a+f)} & \frac{1}{c} \\ \frac{-h}{(a+f)} & 0 & \frac{-d}{(a+f)} & 0 & \frac{-1}{(a+f)} & 0 \\ 0 & 1 & 0 & 0 & 0 & 0 \\ 0 & \frac{-(h+g)}{b} & -0.5 & \frac{1}{b} & 0 & 0 \\ 0 & \frac{(h+g)}{b} & -0.5 & \frac{-1}{b} & 0 & 0 \end{bmatrix} \cdot \begin{bmatrix} 0 \\ 0 \\ 0 \\ 0 \\ My \\ 0 \end{bmatrix} \quad \ldots\ldots\ldots\ldots (3.8)$$

$$F_1 = \frac{1}{2(a+f)} M_y$$

$$F_2 = \frac{1}{2(a+f)} M_y$$

$$F_3 = \frac{-1}{(a+f)} M_y$$

f) When a moment M_z is applied

The sensing elements for the M_z sensor are the cantilever beams CB_1 and CB_2. When the moment M_z is applied, the cantilever beams CB_1 and CB_2 reacts a force F_1 and F_2 respectively through the rigid connecting rods. The other beams have no reaction. Therefore

$$F_3 = F_4 = F_5 = F_6 = 0$$

Then reaction forces are obtained from eqn. (3.3) by substituting only M_z.

$$\begin{Bmatrix} F_1 \\ F_2 \\ F_3 \\ F_4 \\ F_5 \\ F_6 \end{Bmatrix} = \begin{bmatrix} \frac{(a+f+h)}{2(a+f)} & 0 & \frac{d}{2(a+f)} & 0 & \frac{1}{2(a+f)} & \frac{-1}{c} \\ \frac{(a+f+h)}{2(a+f)} & 0 & \frac{d}{2(a+f)} & 0 & \frac{1}{2(a+f)} & \frac{1}{c} \\ \frac{-h}{(a+f)} & 0 & \frac{-d}{(a+f)} & 0 & \frac{-1}{(a+f)} & 0 \\ 0 & 1 & 0 & 0 & 0 & 0 \\ 0 & \frac{-(h+g)}{b} & -0.5 & \frac{1}{b} & 0 & 0 \\ 0 & \frac{(h+g)}{b} & -0.5 & \frac{-1}{b} & 0 & 0 \end{bmatrix} . \begin{bmatrix} 0 \\ 0 \\ 0 \\ 0 \\ 0 \\ Mz \end{bmatrix} \quad \ldots\ldots\ldots\ldots (3.9)$$

$$F_1 = \frac{-1}{c} M_z$$

$$F_2 = \frac{1}{c} M_z$$

3.1.4 Design of the Sensing Elements

The sening elements of the sensor body are designed based on the bending beam theory.

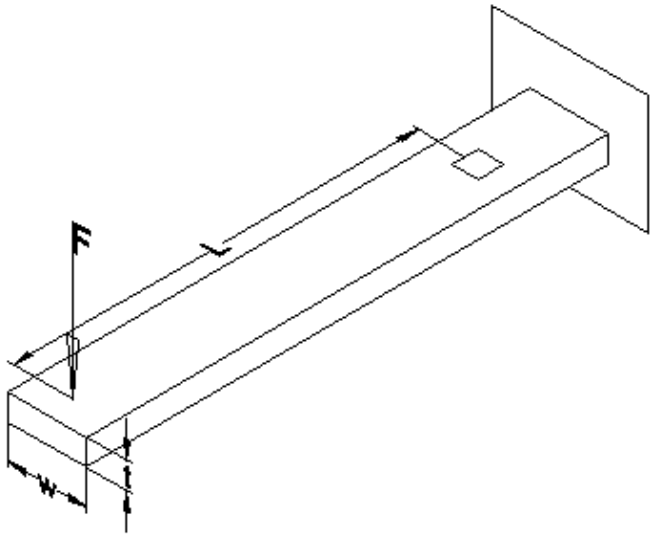

Figure 3.3 Cantilever Beam

For a cantilever beam loaded with a force **F** and has cross section, width *w* and thickness *t*, the bending stress σ_b at a distance *L* from the applied force **F** is given as

$$\sigma_b = \frac{Mc}{I} \quad \text{..... (3.10)}$$

Where σ_b = bending stress

$M = F_i x L_i$ (bending moment at length L from the load application point)

$c = t/2$ (the distance from the neutral axis to the upper or lower surface)

$I = wt^3/12$ (moment of inertia)

Substituting these values eqn. (3.10) can be rewritten as

$$\sigma_b = \frac{6FL}{wt^2} \quad \text{..... (3.11)}$$

By virtue of Hook's Law stress can also be expressed as

$$\sigma = \varepsilon E \quad \text{..... (3.12)}$$

Equating eqn. (3.11) and eqn. (3.12) the theoretical strain (ε) at the surface of the cantilever beam can be expressed as

$$\varepsilon_i = \frac{6F_{iL_i}}{Ew_i t_i^2} \qquad \ldots\ldots\ldots\ldots\ldots\ldots\ldots\ldots\ldots\ldots \qquad (3.13)$$

where i=1,6 (strain for cantilever beams 1 to 6)

The force $\mathbf{F_i}$ for each cantilever beam is obtained when a force or a moment is applied at coordinate OXYZ and is calculated based on eqn. (3.3)

a. Sizing the sensing elements

The dimensions of the cantilever beams (sensing elements), i.e. length *l*, width *w*, and thickness *t* should be determined based on the maximum load condition and the design requirement of the sensor. To do this we have to know the maximum possible force each cantilever beam (sensing elements) can react. This can be obtained from eqn. (3.3) when all forces and moments are applied simultaneously and by assuming some value for *a, b, c, d, f, g* and *h* and specifying the design load values. Based on this the following design requirements and assumed values are used.

The design variables of the modeled six component force/moment sensor are

- The size of the sensor (Length (**L**), Width (**W**), Height (**H**) and Thickness (**T**))

- The rated load (F_x, F_y, F_z, M_x, M_y, M_z) and output of each sensor

-The sizes of the sensing elements of the cantilever beams CB_1 to CB_6 (L_i, w_i, t_i , i=1,6)

- The distances between the load application point and the reaction forces (*a, b, c, d, f, g, h*)

Some of the design variables can be preset by considering the overall size of the sensor and the spacing between the cantilever beams. Based on this the following design variables are preset.

Capacities: $F_Z = F_X = F_Y = N = 3.0$ N., $M_X = M_Y = M_Z = M = 60$Nmm

Dimensions: Maximum distance between sensor and reference point, h = 100 mm

Maximum transducer dimensions: Length (**L**): 180 mm, Width (**W**): 130 mm, Height (H): 130 mm and Thickness (**T**): 1.5 mm.

The maximum size limit force transducer spacing among themselves are chosen to be

a = 80 mm, b = 120 mm, c =100 mm, d = 40 mm, f = 25 mm and g = 45 mm.

Using these values in eqn. (3.3) we can calculate the maximum forces each cantilever beam (sensing elements) can react when all the forces and moments applied simultaneously. This can be summarized in tabular form as follows.

Table 3.3 Maximum possible reactions

N	F_x	F_y	F_z	M_x	M_y	M_z	Σ F (N)
F_1	3.375	0	0.75	0	0.375	0.6	5.1
F_2	3.375	0	0.75	0	0.375	0.6	5.1
F_3	3.75	0	1.5	0	0.75	0	6.0
F_4	0	3.0	0	0	0	0	3.0
F_5	0	3.0	1.5	0.5	0	0	5.0
F_6	0	3.0	1.5	0.5	0	0	5.0

To determine the dimensions of the sensing elements we first calculate the maximum strain at the measuring point bending stress. For this we go from where the strain gauge technology for

maximum linearity reasons selected measuring points elongation of 0.15% and maintained for Aluminum (E = 69,000 N / mm ²). Using the bending stress equation the maximum stress is

$$\sigma_b = \varepsilon.E = 103.5 \text{ N/mm}^2 \text{ …….. (3.14)}$$

We select all the sensing elements along the width to be 24 mm except sensing element 4 which has 13 mm width. All the sensing elements are also milled from a thickness of 1.0 mm.

Thus we are able to calculate the section modules (S):

$$S = \frac{wt^2}{6} \text{ ……. (3.15)}$$

Since the width and thickness of all the sensing elements are equal, except sensing element 4, their section modules are equal.

Thus

$$S_1 = S_2 = S_3 = S_5 = S_6 = \frac{wt^2}{6} = \frac{24x1^2}{6} \text{mm}^3 = 4.0 \text{ mm}^3$$

And $$S_4 = \frac{wt^2}{6} = \frac{13x1^2}{6} \text{mm}^3 = 2.167 \text{ mm}^3$$

With the previously computed allowable bending stress (eqn. 3.14), we get over the following permissible bending moments:

$$M_b = \sigma_b.S_b \text{ …….. (3.16)}$$

Thus,

$$M_1 = M_2 = M_3 = M_5 = M_6 = \sigma_b.S_b = (103.5 \text{ N/mm}^2) \text{ x } (4.0\text{mm}^3) = 414 \text{ Nmm}$$

And $$M_4 = \sigma_b.S_b = (103.5 \text{ N/mm}^2) \text{ x } (2.167\text{mm}^3) = 224.25 \text{ Nmm}$$

$$\text{And } M_4 = 224.25 \text{ Nmm}$$

Then we can obtain the lengths of the sensing elements (cantilever beams) as:

$$l_i = \frac{M_{bi}}{F_i} \quad \text{..... (3.17)}$$

We have already calculated $\mathbf{F_i}$ values for all sensing elements in Table 3.3 above and therefore we can calculate the length of each sensing element as:

$l_1 = \frac{M_{b1}}{F_1} = \frac{414\ Nmm}{5.1\ N}$ = 81.18 mm

$l_2 = \frac{M_{b2}}{F_2} = \frac{414\ Nmm}{5.1\ N}$ = 81.18 mm

$l_3 = \frac{M_{b3}}{F_3} = \frac{414\ Nmm}{6.0\ N}$ = 69.0 mm

$l_4 = \frac{M_{b4}}{F_4} = \frac{224.25\ Nmm}{3.0\ N}$ = 74.75 mm

$l_5 = \frac{M_{b5}}{F_5} = \frac{414\ Nmm}{5.0\ N}$ = 82.8 mm

$l_6 = \frac{M_{b5}}{F_5} = \frac{414\ Nmm}{5.0\ N}$ = 82.8 mm

All the dimensions can be summarized in table form as follows

Table 3.4 Summary of design data

S. No.	Force , F_i (N)	Section Modulus , S (mm^3)	Moment , M (Nmm)	Length , *l* (mm)
1	5.1	4.000	414.00	81.18 ≈ 81
2	5.1	4.000	414.00	81.18 ≈ 81
3	6.0	4.000	414.00	69 = 69
4	3.0	2.167	224.25	74.75 ≈ 75
5	5.0	4.000	414.00	82.8 ≈ 83
6	5.0	4.000	414.00	82.8 ≈ 83

Based on the calculated design data the detail 2D and 3D drawings of the sensor are prepared.

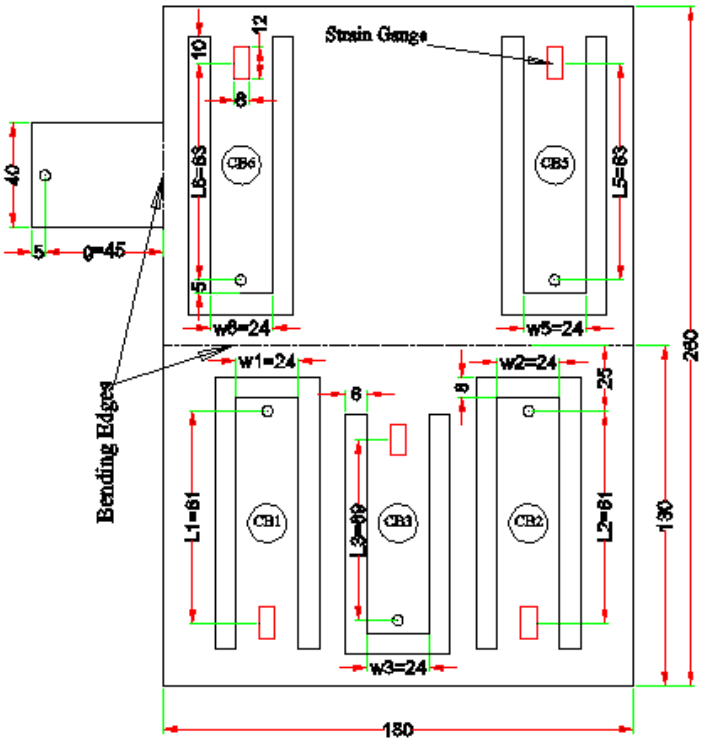

(a) Upper half

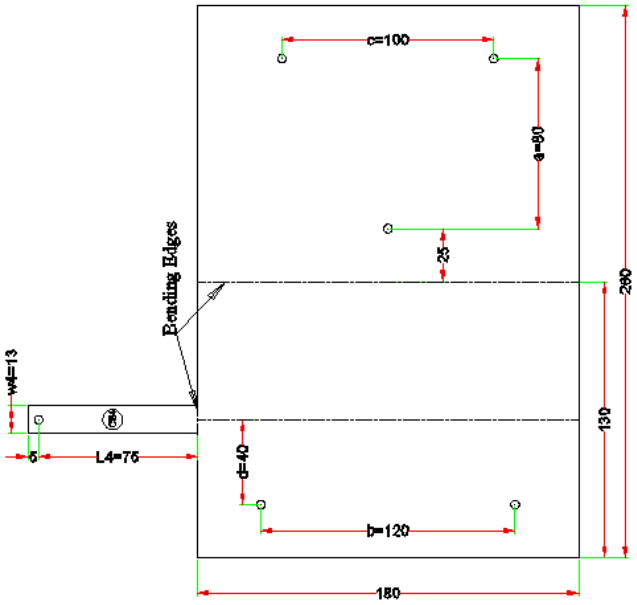

(b) Lower half

Note: All Dimensions are in mm

Figure 3.4 Detail dimension for 2D drawing of the two half plates before bending

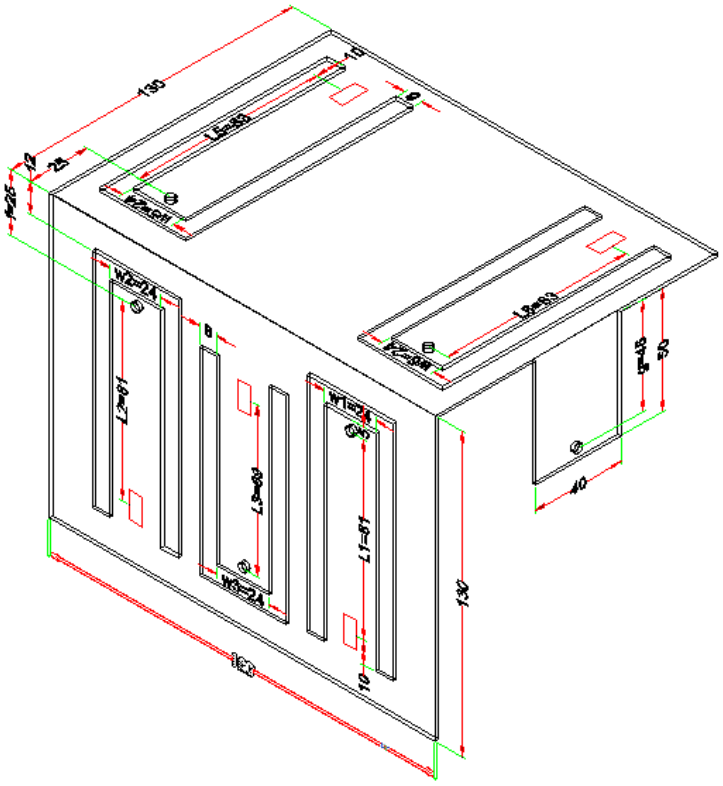

(a) upper half

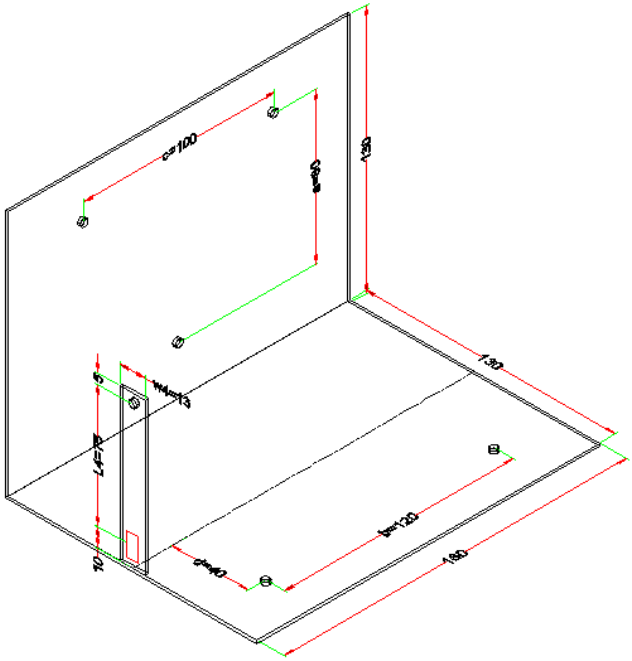

(b) lower half

Figure 3.5 3D drawing of the two halve plates after bending

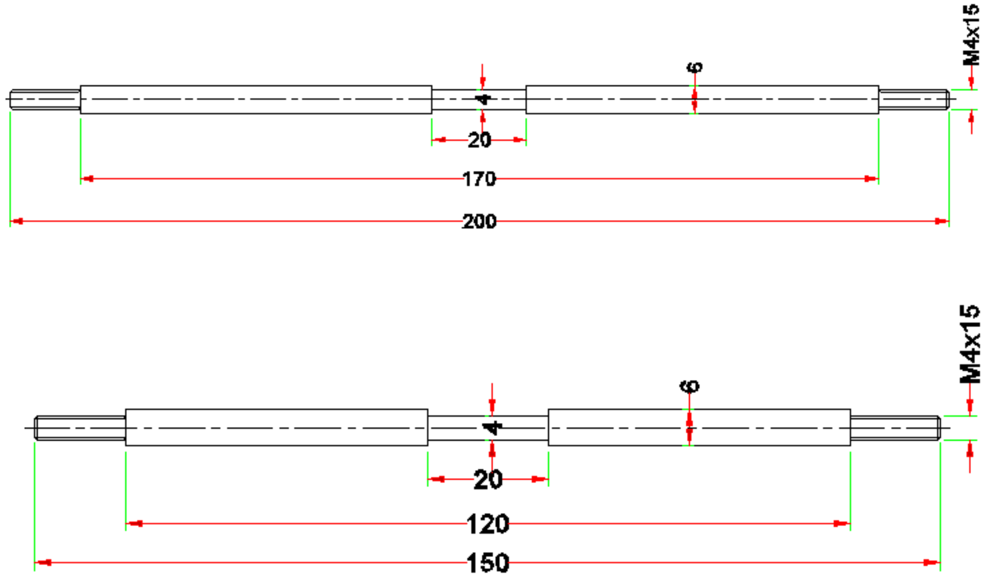

Figure 3.6 Connecting rods

b. Calibration Matrix

Consider a structure (figure 3.1) which is loaded (input) at coordinate OXYZ by an unknown force vector, **F** = (F_x, F_y, F_z, M_x, M_y, M_z) in its linear range. Then, on the surface of the structure there must produce (output) vector of n strain signals, S = (S1; S2; S3; . . . ; Sn) in the prescribed measurement locations. The superposition principle of linear elasticity then provides the following linear relationship:

$$S = [C].F \quad \ldots\ldots\ldots\ldots\ldots\ldots\ldots\ldots \quad (3.18)$$

Where [C] is an n x 6 strain compliance matrix, with its entries in each column being the strains induced by a unit force for each corresponding force component in the strain measurement locations.

For n <= 6, the solution for the force vector is directly obtained by a matrix inversion operation on eqn. (3.18)

$$\mathbf{F} = [C]^{-1}.S = [A].S \quad \ldots\ldots\ldots\ldots\ldots\ldots\ldots\ldots \quad (3.19)$$

The matrix [A] here is the calibration matrix of the sensor, which represents a matrix that directly multiplies the strain signal vector (output) to obtain the to-be-measured force vector (input).

In our case n = 6 so that the direct matrix inversion can be applied. But when we compare eqn. (3.19) with eqn. (3.2), we can observe that eqn. (3.19 is equivalently expressed as eqn. (3.2) so that we can directly obtain the calibration matrix [A] from eqn. (3.2) by expressing the right part of eqn. (3.2) in terms of strain and its coefficient matrix which is equivalent to the calibration matrix [A] as follows.

$$[A]=\begin{bmatrix} 3.41 & 3.41 & 4.00 & 0 & 0 & 0 \\ 0 & 0 & 0 & 1.99 & 0 & 0 \\ 0 & 0 & 0 & 0 & -3.33 & -3.33 \\ 0 & 0 & 0 & 238.8 & 199.8 & -199.8 \\ -341.0 & -341.0 & -720.0 & 0 & 133.2 & 133.2 \\ -170.5 & 170.5 & 0 & 0 & 0 & 0 \end{bmatrix} x10^3 \quad \ldots\ldots. (3.20)$$

With the calibration matrix [A] being available, the force vector **F** can be expressed as:

$$\mathbf{F} = [A].[s] = \begin{bmatrix} 3.41 & 3.41 & 4.00 & 0 & 0 & 0 \\ 0 & 0 & 0 & 1.99 & 0 & 0 \\ 0 & 0 & 0 & 0 & -3.33 & -3.33 \\ 0 & 0 & 0 & 289.0 & 199.8 & -199.8 \\ -341.0 & -341.0 & -820.0 & 0 & 133.2 & 133.2 \\ -170.5 & 170.5 & 0 & 0 & 0 & 0 \end{bmatrix} x10^3 . \begin{bmatrix} \varepsilon_1 \\ \varepsilon_2 \\ \varepsilon_3 \\ \varepsilon_4 \\ \varepsilon_5 \\ \varepsilon_6 \end{bmatrix} \ldots\ldots (3.21)$$

In expanded scalar forms, the forces and moments are

$F_x = (3.41\varepsilon_1 + 3.41\varepsilon_2 + 4.0\varepsilon_3)\ x\ 10^3]$ [N] …… …… (3.21a)

$F_y = 1.99\ x(\varepsilon_4)\ x10^3$ [N] …… ……..…….. (3.21b)

$F_z = -3.33\ x\ (\varepsilon_5 + \varepsilon_6)\ x\ 10^3$ [N] …… ……..….. (3.21c)

$M_x = (289.0\varepsilon_4 + 199.8\varepsilon_5 - 199.8\varepsilon_6)\ x10^3$ [Nmm] …… ….……. (3.21d)

$M_y = (-341.0\varepsilon_1 - 341.0\varepsilon_2 - 820.0\varepsilon_3 + 133.2\varepsilon_5 + 133.2\varepsilon_6)\ x10^3$ [Nmm] …… (3.21e)

$M_z = (-170.5\varepsilon_1 + 170.5\varepsilon_2)\ x\ 10^3$ [Nmm] ……..…….. (3.21f)

The elements of the strain signal vector S can be obtained in two methods. The first method is using the application of electrical circuits. The appropriate electrical circuit commonly used for this application is wheat stone bridge circuit. For this specific work i.e. plate cantilever beam, half bridge circuit is used. The equation for calculating the strain for half bridge circuit is given as

$$\varepsilon_i = \frac{2V_o}{GF.V_i} \quad \text{..... (3.22)}$$

The second method is using an instrument which can directly measure strain. In this work we use model P-3500 strain indicator to read the strain produced on the surface of the sensing elements.

3.2Fabrication of the sensor

The sensor body is fabricated from Aluminum sheet with 1.5 mm thickness using a milling machine and hydraulic bending machine. The size of the sensor is based on the design parameters obtained in the previous chapter. It is made from two 90^o bend plates which are connected each other with steel bars. An inbuilt cantilever beam sensing elements are milled on the surface of the plates. The sensor consists of a total of six sensing elements. The lower half has only one sensing element while the remaining five are made on the upper half.

a) Lower half b) Upper half

Figure 3.7 The two halves of the fabricated sensor

The two halves are connected to each other to make a rectangular box with threaded steel bars and nuts.

Figure 3.8 Connecting bars with nuts

3.2.1 Strain Gauge Installation and wiring

After the sensor body is fabricated the strain gauges are attached on the sensing elements whose positions of attachment are already determined in the previous chapter.

i) Strain Gauge Installation

Strain gauges (SG) are designed to measure strains. The results of such measurements can be used to make statements about the material stress of the measurement object, about the nature and amount of forces acting on the measurement object, etc. A strain gauge can only perform the required task if the strain to be measured is transferred faultlessly and without loss. This requires an intimate

connection between the strain gauge and the measurement object. The required intimate, full contact connection between the measurement object and SG can only be achieved with special adhesives and methods.

In this project the following methods are applied in order to get faultless measurement as much as possible.

a) Strain gauge preparation

The strain gauge that is going to be used in this project is a foil type strain gauge made by HBM Company.

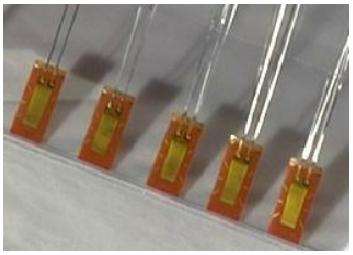

Figure 3.9 Foil Strain Gauge

- It is first cleaned with cotton bud soaked in a solvent called RMS1 in order to remove finger print or any other contamination on the bonding side of the strain gauge.
- The solder terminal is cut at the required length and cleaned with glass fiber brush and solvent

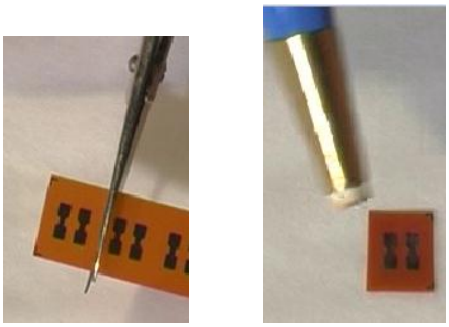

Figure 3.10 Solder Terminal preparations

- Then the strain gauge and the solder terminal are connected using adhesive tape.

b) Bonding surface preparation

The main objective of bonding surface preparation is to create a surface without pores, notches and oxides, not too rough and easily wetted. In order to get this condition the following preparation stages are used.

Course Cleaning:

It is used to remove impurities, lubricants and grease layers around the measurement point. The cleaning process is held by using a cellulose pad deep in to a solvent. The solvent used in this process is called RMS1.

Roughening:

The adhesion of bonded parts is based on the adhesion between the adhesive and the surface wetted by the adhesive. Adhesion is mainly based on the attractive forces between neighboring molecules. An increase in bonding force is only possible by increasing the contact surfaces. This can only be achieved by roughening.

The recommended roughening material for aluminum is emery paper (sand paper) with grain size P220. The roughening process is done in a circular motion in order to avoid directional biases.

Figure 3.11 P220 Sand paper

Cleaning:

In this step dusts created during roughening process are cleaned using cellulose pad deep in to RMS1 solvent. The cleaning process is repeated until the surface becomes completely clean.

Marking:

Marking is made in order to alien the taste object to the strain gauge's center mark. For this purpose an empty ball point pen is used.

Fine Cleaning:

This is the last step of bonding surface preparation and is done to be sure that any dust or contamination is removed on the bonding surface.

c) Strain gauge bonding

After the surface preparation is completed the bonding process continued. The adhesive type used in this work is Z70 super glue. It is low-viscosity cyano-acrylate adhesive, which dries in seconds. The bonding process is done by putting one drop of Z70 adhesive on the bonding side of the strain gauge and evenly distributing through the bonding surface. Then using a thumb the strain gauge is pressed down on the taste object for about one minuet. This is the curing period of the Z70 adhesive.

ii) Soldering and wiring

The strain gauges used in this work has no connecting strips. So it is necessary to solder a connecting strip to connect the strain gauge with the solder terminal. Here it is better to use a strain gauge which has connecting strip together to prevent the strain gauge from damage when trying to solder.

Based on this the soldering process is conducted to connect the strain gauge with the solder terminal. Two lead wires are also soldered on the solder terminal as positive and negative terminal.

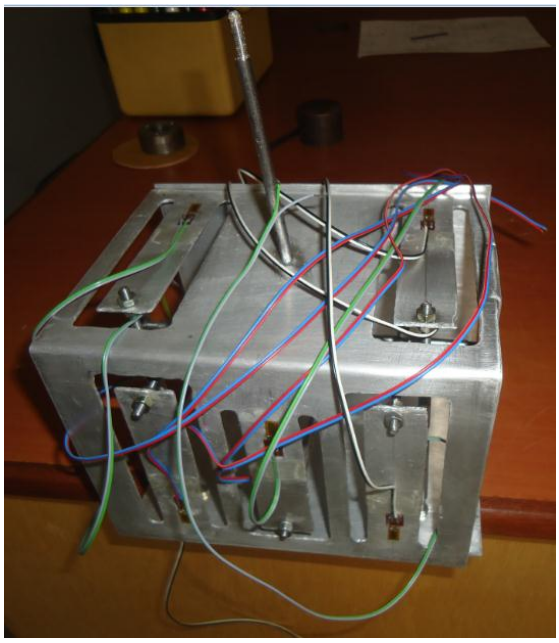

Figure 3.12 Fabricated Six component force /moment sensor

After soldering the wires the strains are measured using an instrument called P-3500 strain indicator which can directly measure strain in micro level.

3.2.2 Strain Measuring Instrument

In this work a Model P-3500 Strain Indicator is used for the strain read out. The Model P-3500 Strain Indicator is a portable, battery-powered instrument with unique features for use in stress analysis testing, and for use with strain gage based transducers. In use, the operator follows a logical sequence of setup steps by activating color-coded pushbutton controls to prepare the instrument for making accurate and reliable measurements.

TheP-3500 also incorporates a highly stable DC amplifier, precisely regulated bridge excitation supply, and precisely settable gage factor controls.

Static measurements are displayed directly on the indicator's readout with 1 micro-strain resolution. The instrument will accept full-, half-, or quarter-bridge strain gage inputs, and all required bridge completion components for 120, 350 and 1000 ohm gages are built in.

Gage factor is precisely settable (to a resolution of 0.001) by a front-panel 10-turn potentiometer, and is displayed on the digital readout when the gage factor push button is depressed. However, when the MULT push button is set to the X10 position, the gauge factor range is effectively multiplied by 10.

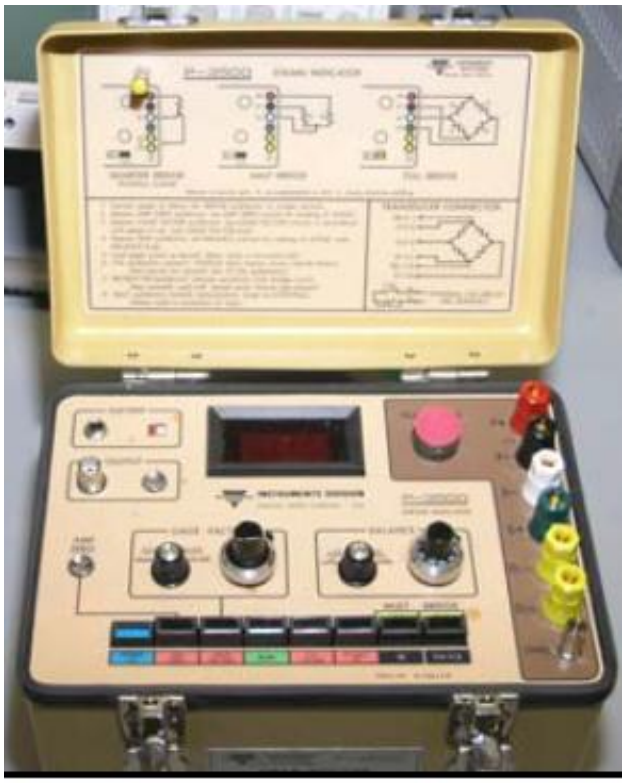

Figure 3.13 Model P-3500 Strain Indicator

CHAPTER FOUR

EXPERIMENTAL RESULT AND DISCUSIION

4.1 Experimental Testing

In the previous chapter the sensor body is designed and fabricated based on the design data. In this chapter an experimental test is carried out and the result is discussed by comparing with the theoretical values.

4.1.1 Experimental test set up

To apply a force/moment on the sensor body a test set up should be prepared. The set up should be made for the application of each force/moment. First of all the sensor body should be in equilibrium. To do this the sensor is securely attached on the table. The required amount of force/moment is applied using known masses. Then the strain on each sensing element is registered. The figure below shows the set up for the application of each force/moment.

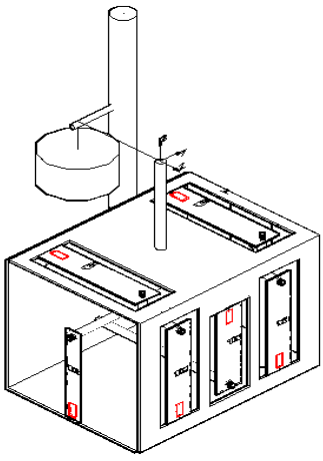

a) When a force Fx is applied

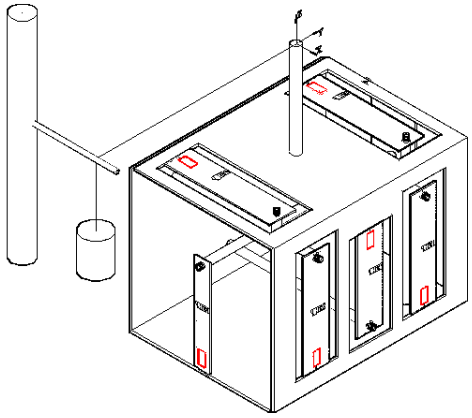

b) When a force Fy is applied

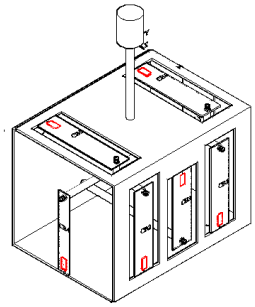

c) When a force Fz is applied

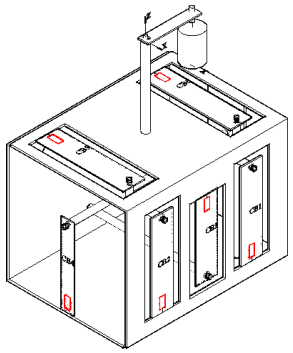

d) When a Moment Mx is applied

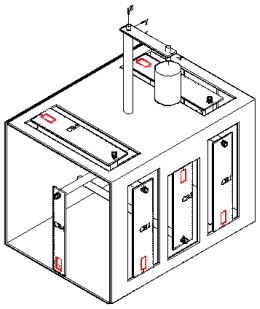

e) When a Moment My is applied

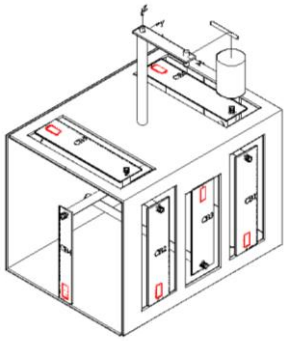

f) When a Moment Mz is applied

Figure 4.1 Forces and Moments Applying Position

Three masses are used in this test. The masses are first measured with digital balance which has four digit accuracy and multiplied by gravitational constant g = 9.81 m/s^2. The length of the moment arm (**r**) used to create the required moment is 50 mm.

Table 4.1 Test masses

S. No.	Known mass (kg.)	Weight (W) = m x g (N)
1	0.1371	1.35
2	0.1534	1.51
3	0.2832	2.78

The experiment is carried out three times for each force and moment using the above mentioned known masses. The results obtained during the experiment are summarized in the next section.

4.1.2 Experimental Results

Using the above measured masses the required forces/ moments are applied at coordinate point OXYZ as the test set up indicates and the reaction forces at each cantilever beam (sensing element) are obtained according to eqn. (3.3) as follows.

Table 4.2 When F = 1.35 N, M = 67.5 Nmm and r = 50mm.

F (N)	Fx = 1.35N	Fy = 1.35N	Fz = 1.35N	Mx = 67.5 Nmm	My = 67.5 Nmm	Mz = 67.5 Nmm	ΣF (N)
F1	1.32	0	0.26	0	0.32	-0.68	2.58
F2	1.32	0	0.26	0	0.32	0.68	2.58
F3	-1.29	0	-0.51	0	-0.64	0	2.44
F4	0	1.35	0	0	0	0	1.35
F5	0	-1.63	0.68	0.56	0	0	2.87
F6	0	1.63	0.68	-0.56	0	0	2.87

Table 4.3 When F = 1.51N, M = 75.5 Nmm and r = 50mm.

F (N)	Fx = 1.51 N	Fy = 1.51 N	Fz = 1.51 N	Mx = 75.5 Nmm	My = 75.5 Nmm	Mz = 75.5 Nmm	ΣF (N)
F1	1.47	0	0.29	0	0.36	-0.76	2.88
F2	1.47	0	0.29	0	0.36	0.76	2.88
F3	-1.44	0	-0.58	0	-0.72	0	2.74
F4	0	1.51	0	0	0	0	1.51
F5	0	-1.83	0.76	0.63	0	0	3.22
F6	0	1.83	0.76	-0.63	0	0	3.22

Table 4.4 When F = 2.78N, M = 139 Nmm and r = 50mm.

F (N)	Fx = 2.78 N	Fy = 2.78 N	Fz = 2.78 N	Mx = 139 Nmm	My = 139Nmm	Mz = 139 Nmm	ΣF (N)
F1	2.71	0	0.53	0	0.66	-1.39	5.29
F2	2.71	0	0.53	0	0.66	1.39	5.29
F3	-2.65	0	-1.06	0	-1.32	0	5.03
F4	0	2.78	0	0	0	0	2.78
F5	0	-3.36	-1.39	1.16	0	0	5.91
F6	0	3.36	-1.39	-1.16	0	0	5.91

Using the above reaction forces the theoretical strains for each sensing elements are calculated based on eqn. (3.13) and obtained as follows.

I. Theoretical Strain Values

The theoretical strains for the applied forces and moments are calculated from the reaction forces on each sensing element.

Table 4.5 When F = 1.35N, M = 67.5 Nmm and r = 50mm. (Experiment I)

E ($x10^{-6}$)	Fx = 1.35 N	Fy = 1.35 N	Fz = 1.35 N	Mx = 67.5 Nmm	My = 67.5 Nmm	Mz = 67.5 Nmm
ε_1	387.4	0	76.3	0	93.9	-199.6
ε_2	387.4	0	76.3	0	93.9	199.6
ε_3	-322.5	0	-127.5	0	-160	0
ε_4	0	677.3	0	0	0	0
ε_5	0	-490.2	204.5	168.4	0	0
ε_6	0	490.2	204.5	-168.4	0	0

Table 4.6 When F = 1.51N, M = 75.5 Nmm and r = 50mm. (Experiment II)

E ($x10^{-6}$)	Fx = 1.51 N	Fy = 1.51 N	Fz = 1.51N	Mx = 75.5 Nmm	My = 75.5 Nmm	Mz = 75.5 Nmm
ε_1	431.4	0	85.1	0	105.7	-223
ε_2	431.4	0	85.1	0	105.7	223
ε_3	-360	0	-145	0	-180	0
ε_4	0	757.5	0	0	0	0
ε_5	0	-550.3	228.6	189.5	0	0
ε_6	0	550.3	228.6	-189.5	0	0

Table 4.7 When F = 2.78N, M = 139 Nmm and r = 50mm. (Experiment III)

E ($x10^{-6}$)	Fx = 2.78 N	Fy = 2.78 N	Fz = 2.78 N	Mx = 139 Nmm	My = 139 Nmm	Mz = 139 Nmm
ε_1	795.3	0	155.5	0	193.7	-407.9
ε_2	795.3	0	155.5	0	193.7	407.9
ε_3	-662.5	0	-265	0	-330	0
ε_4	0	1267.5	0	0	0	0
ε_5	0	-1010.4	418.0	348.8	0	0
ε_6	0	1010.4	418.0	-348.8	0	0

At the same time the experimental strains measured by P-3500 strain indicator when each forces and moments are applied are obtained as follows.

II. Experimental Strain Values

Table 4.8: When F = 1.35N, M = 67.5 Nmm and r = 50mm. (Experiment I)

ε ($x10^{-6}$)	Fx = 1.35N	Fy = 1.35 N	Fz = 1.35 N	Mx = 67.5 Nmm	My = 67.5 Nmm	Mz = 67.5 Nmm
ε_1	269	0	51	0	69	-140
ε_2	263	0	57	0	62	136
ε_3	-231	0	-88	0	-110	0
ε_4	0	414	0	0	0	0
ε_5	0	-292	171	106	0	0
ε_6	0	290	161	-114	0	0

Table 4.9: When F = 1.51N, M = 75.5 Nmm and r = 50mm. (Experiment II)

ε ($x10^{-6}$)	Fx = 1.51 N	Fy = 1.51N	Fz = 1.51 N	Mx = 75.5 Nmm	My = 75.5 Nmm	Mz = 75.5 Nmm
ε_1	321	0	64	0	72	-144
ε_2	308	0	65	0	67	148
ε_3	-244	0	-105	0	-117	0
ε_4	0	462	0	0	0	0
ε_5	0	-346	182	121	0	0
ε_6	0	340	175	-127	0	0

Table 4.10: When F = 2.78N, M = 139 Nmm and r = 50mm. (Experiment III)

ε($x10^{-6}$)	Fx = 2.78 N	Fy = 2.78 N	Fz = 2.78 N	Mx = 139 Nmm	My = 139Nmm	Mz = 139 Nmm
ε_1	522	0	102	0	125	-269
ε_2	530	0	109	0	128	259
ε_3	-424	0	-181	0	-210	0
ε_4	0	849	0	0	0	0
ε_5	0	-628	307	227	0	0
ε_6	0	639	301	-230	0	0

4.2 Discussing Results

In the previous section the sensor body was designed based on the proposed equilibrium equation, manufactured and tasted. The test is carried out using three different masses and the corresponding theoretical and experimental results were obtained. In this section the experimental results will

discuss by comparing with the theoretical results which are calculated based on the proposed equations.

4.2.1 Comparison of strains

From the previous test of the first experiment the reaction forces F_1, F_2, F_3, F_4, F_5 and F_6 are calculated based on eqn. (3.3) when $F_x = F_y = F_z = 1.35$N. and $M_x = M_y = M_z = 67.5$Nmm. are applied and their values are displayed on Table 4.2. Using these reaction forces in eqn. (3.13) the corresponding theoretical strain are calculated and their values are displayed on Table 4.5. At the same time the experimental strains directly read from strain indicator, when each load is applied in the first experiment, is displayed on table 4.8. Now let us compare the experimental and theoretical strain results.

Table 4.11 Comparison of theoretical and experimental strain results

E ($x10^{-6}$)		Fx = 1.35 N	Fy = 1.35 N	Fz = 1.35 N	Mx = 67.5 Nmm	My = 67.5 Nmm	Mz = 67.5 Nmm
ε_1	Theo.	387.4	0	76.3	0	93.9	-199.6
	Exp.	269	0	51	0	69	-140
	Error	30.6%	-	33.2%	-	26.5%	29.9%
ε_2	Theo.	387.4	0	76.3	0	93.9	199.6
	Exp.	263	0	57	0	62	136
	Error	32.1%	-	25.3%	-	34.0%	31.9%
ε_3	Theo.	-322.5	0	-127.5	0	-160	0
	Exp.	-231	0	-88	0	-110	0
	Error	28.4%	-	31.0%	-	31.3%	-
ε_4	Theo.	0	677.3	0	0	0	0
	Exp.	0	414	0	0	0	0
	Error	-	38.9%	-	-	-	-
ε_5	Theo.	0	-490.2	204.5	168.4	0	0
	Exp.	0	-292	171	106	0	0
	Error	-	40.4%	16.4%	37.1%	-	-
ε_6	Theo.	0	490.2	204.5	-168.4	0	0
	Exp.	0	290	161	-114	0	0
	Error	-	40.8%	21.3%	32.3%	-	-

The above Table shows the rated strain, the theoretical strain and their corresponding error when each forces and moments are applied in the first experiment.

As it is stated in chapter three the sensing elements when F_x is applied are cantilever beams CB_1, CB_2 and CB_3 and their corresponding strains are ε_1, ε_2 and ε_3. The theoretical strain for ε_1 and ε_2 is 387.4μm/m and the experimental strain directly read from the strain indicator for ε_1 is 269μm/m. and for ε_2 is 263μm/m. Therefore the error for the sensing element ε_1 is 30.6% and ε_2 is 32.1%. The theoretical strain for ε_3 is -322.5μm/m and the experimental strain directly read from the strain indicator is -231μm/m. Therefore the error for the sensing element ε_3 is 28.4%.

The sensing elements when F_y is applied are cantilever beams CB_4, CB_5 and CB_6 and their corresponding strains are ε_4, ε_5 and ε_6. The theoretical strain for ε_4 is 677.3μm/m and the experimental strain directly read from the strain indicator is 414μm/m. Therefore the error for the sensing element ε_4 is 38.9%. The theoretical strain for ε_5 and ε_6 is 490.2μm/m and the experimental strain directly read from the strain indicator for ε_5 is 292μm/m. and for ε_6 is 290μm/m. Therefore the error for the sensing element ε_5 is 40.4% and ε_6 is 40.8%.

The sensing elements when F_z is applied are cantilever beams CB_1, CB_2, CB_3, CB_5 and CB_6 and their corresponding strains are ε_1, ε_2, ε_3, ε_5 and ε_6. The theoretical strain for ε_1 and ε_2 is 76.3μm/m and the experimental strain directly read from the strain indicator for ε_1 is 51μm/m. and for ε_2 is 57μm/m. Therefore the error for the sensing element ε_1 is 33.2% and ε_2 is 25.3%. The theoretical strain for ε_3 is -127.5μm/m and the experimental strain directly read from the strain indicator is -88μm/m. Therefore the error for the sensing element ε_3 is 31.0%. The theoretical strain for ε_5 and ε_6

is 204.5μm/m and the experimental strain directly read from the strain indicator for ε_5 is 171μm/m. and for ε_6 is 161μm/m. Therefore the error for the sensing element ε_5 is 16.4% and ε_6 is 21.3%.

The sensing elements when M_x is applied are cantilever beams CB_5 and CB_6 and their corresponding strains are ε_5 and ε_6. The theoretical strain for ε_5 and ε_6 is 168.4μm/m and the experimental strain directly read from the strain indicator for ε_5 is 106μm/m. and for ε_6 is 114μm/m. Therefore the error for the sensing element ε_5 is 37.1% and ε_6 is 32.3%.

The sensing elements when M_y is applied are cantilever beams CB_1, CB_2 and CB_3 and their corresponding strains are ε_1, ε_2 and ε_3. The theoretical strain for ε_1 and ε_2 is 93.9μm/m and the experimental strain directly read from the strain indicator for ε_1 is 69μm/m. and for ε_2 is 62μm/m. Therefore the error for the sensing element ε_1 is 26.5% and ε_2 is 34.0%. The theoretical strain for ε_3 is -160.0μm/m and the experimental strain directly read from the strain indicator is -110μm/m. Therefore the error for the sensing element ε_3 is 31.3%.

The sensing elements when M_z is applied are cantilever beams CB_1 and CB_2 and their corresponding strains are ε_1 and ε_2. The theoretical strain for ε_1 and ε_2 is 199.6μm/m and the experimental strain directly read from the strain indicator for ε_1 is 140μm/m. and for ε_2 is 136μm/m. Therefore the error for the sensing element ε_1 is 29.9% and ε_2 is 31.9%.

The remaining results for experiment two and experiment three of the theoretical and experimental strain values are also displayed on table 5.6 & table 5.9 and table 5.7 & table 5.10 respectively. Their corresponding error can be calculated in the same manner as experiment one.

4.2.2 Comparison of Loads

The main purpose of this study is to design and manufacture the six component force /moment sensor which can measure externally applied unknown loads. So the fabricated sensor should give some amount of result when an external load applied on it. For example when an unknown aerodynamic drag force is applied the sensor should display the value which is believed as a drag force. But in reality it is impossible to measure exactly the unknown external load. There will always be a deviation between the actual externally applied load and the measured load. In this section we will compare the actual external load and the measured load from the experimental results in the previous chapter.

In the previous experiment the three forces and three moments are applied independently on the sensor and their corresponding strains are measured (table 4.8 – table 4.10). The directly applied loads can be compared with the measured loads, which can be obtained in terms of strain using eqn. (21a) to eqn. (21f), in the three experiments and their corresponding error can also be obtained as follows.

Table 4.12 Comparing Actual and measured Forces from the first experiment

	F_x (N)	F_y (N)	F_z (N)	M_x (Nmm)	M_y (Nmm)	M_z (Nmm)
Actual	1.35	1.35	1.35	67.5	67.5	67.5
Measured	0.89	0.823	1.11	44.0	45.53	46.92
Error (%)	34.1	39.0	17.8	34.8	32.5	30.5

Table 4.13 Comparing Actual and measured Forces from the second experiment

	F_x (N)	F_y (N)	F_z (N)	M_x (Nmm)	M_y (Nmm)	M_z (Nmm)
Actual	1.51	1.51	1.51	75.5	75.5	75.5
Measured	1.17	0.92	1.19	45.6	48.54	49.64
Error (%)	22.5	39.1	21.2	39.6	35.7	35.9

Table 4.14 Comparing Actual and measured Forces from the third experiment

	F_x (N)	F_y (N)	F_z (N)	M_x (Nmm)	M_y (Nmm)	M_z (Nmm)
Actual	2.78	2.78	2.78	139	139	139
Measured	1.89	1.69	2.02	91.31	86.95	89.76
Error (%)	32.0	39.2	27.3	34.3	37.4	35.4

The above tabular results can also be compared in graphical form as follows

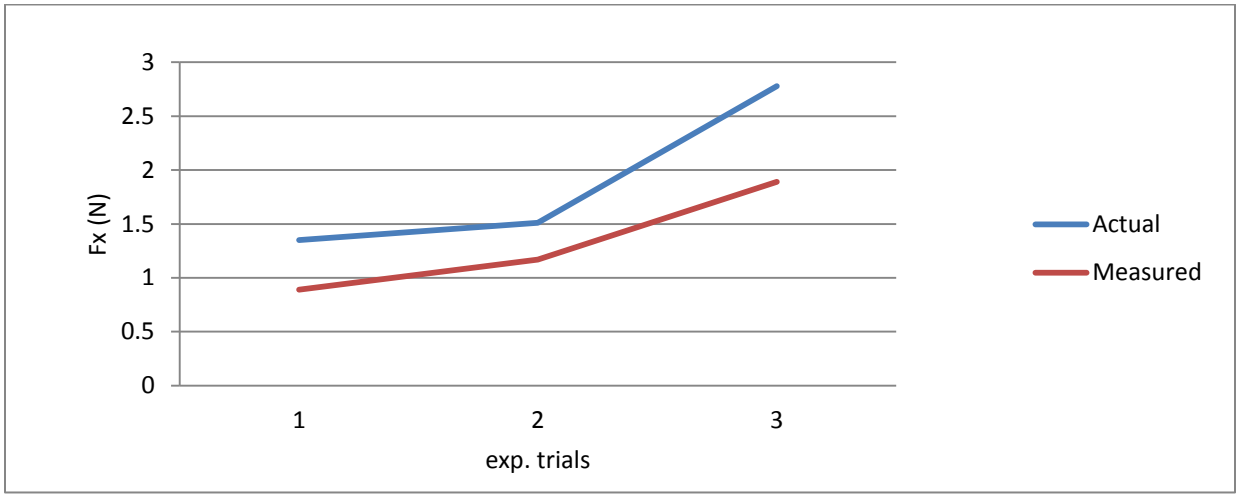

(a)

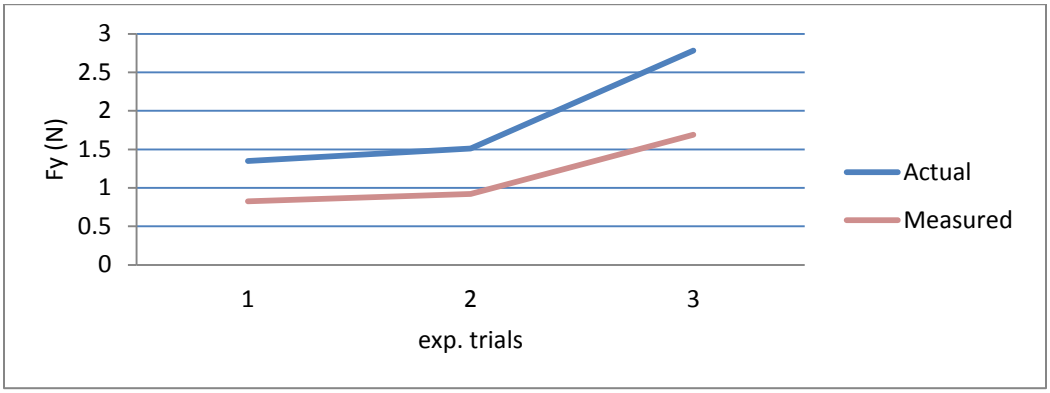
3
2.5
2
1.5
1
0.5
0
Fy (N)
1
2
3
exp. trials
Actual
Measured

(b)

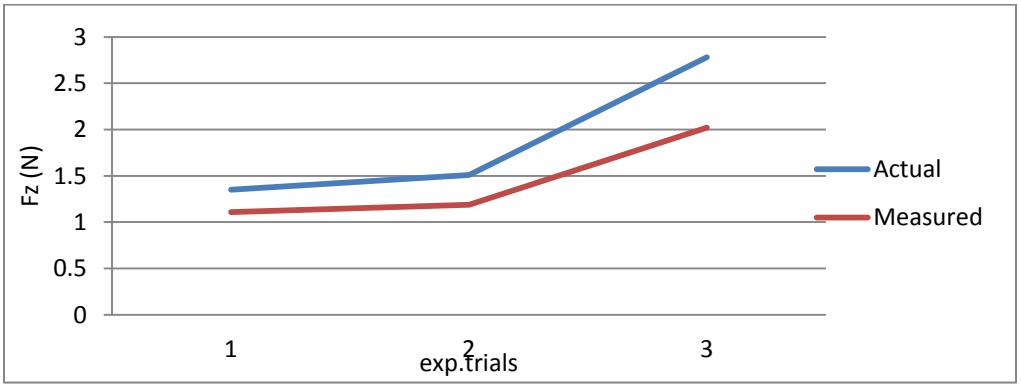
3
2.5
2
1.5
1
0.5
0
Fz (N)
1
2
3
exp.trials
Actual
Measured

(c)

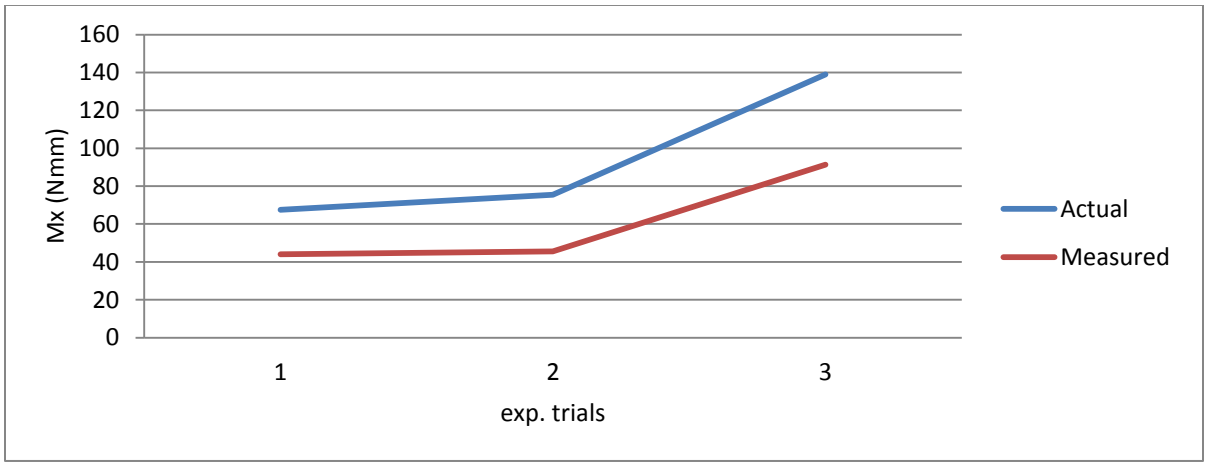
160
140
120
100
80
60
40
20
0
Mx (Nmm)
1
2
3
exp. trials
Actual
Measured

(d)

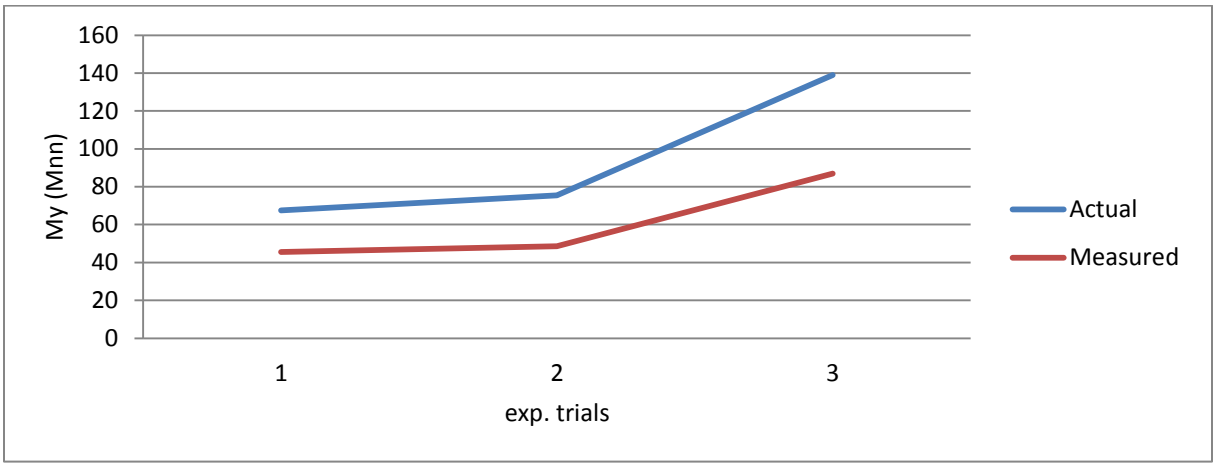

(e)

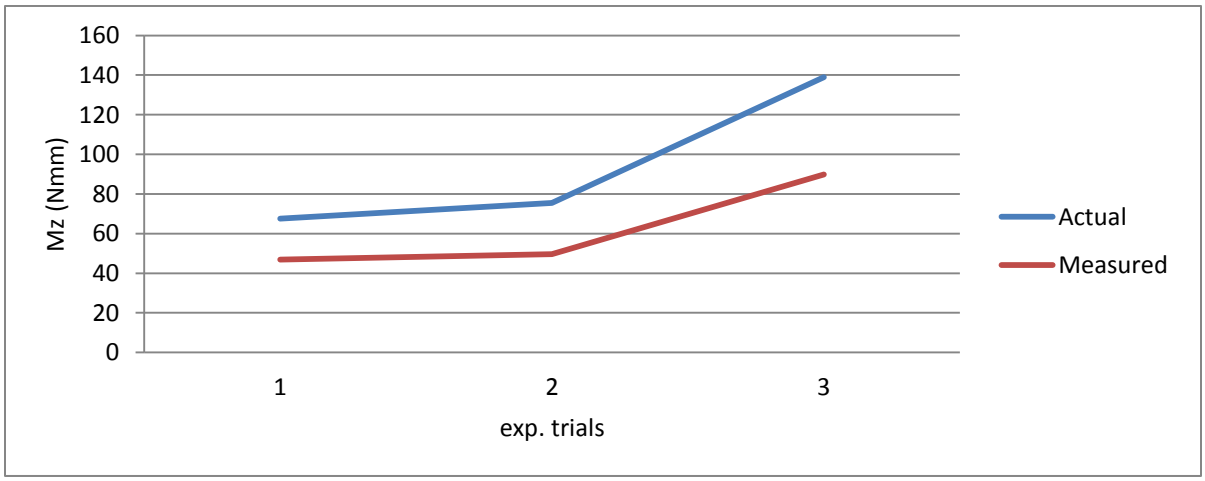

(f)

Figure 4.2 Comparison of Actually Applied loads Vs. Measured loads

From the three tables (table 4.12 – table 4.14) the measured load values and their corresponding errors are displayed for the three different loads. In the first experiment F_x is measured with 34.1% error, in the second experiment it is measured with 22.5% error and finally in the third experiment it is measured with 32% error. So we can summarize the three errors as a single average error of 29.5% and we can also say that F_x is measured with 29.5% error.

In the same way F_y is measured with 39% error in the first experiment, 39.1% error in the second experiment and 39.2% error in the third experiment. So F_y is measured with the average single error of 39.1%. F_z is measured with 17.8% error in the first experiment, 21.2% error in the second experiment and 27.3% error in the third experiment. So F_z is measured with the average single error of 22.1%. M_x is measured with 34.8% error in the first experiment, 39.6% error in the second experiment and 34.3% error in the third experiment. So M_x is measured with the average single error of 36.3%. M_y is measured with 32.5% error in the first experiment, 35.7% error in the second experiment and 37.4% error in the third experiment. So M_y is measured with the average single error of 35.2%. M_z is measured with 30.5% error in the first experiment, 35.9% error in the second experiment and 35.4% error in the third experiment. So M_z is measured with the average single error of 33.9%.

The graphs (a) to (f) also reveal the comparison of actual load Vs. measured load. From the graphs the upper line is the actually applied load and the lower line is the measured load. The space between the two lines is the amount of error in each loading case. From the graphs it is obvious that the larger the space in between, the higher the amount of error and the smaller the space in between implies the smaller the amount of error.

From the above discussion we observe that the average error of all the measured forces and moments is below 40%. The errors are calculated by comparing the actual value with the theoretical result. It is obvious that the errors look larger. However as a first design it is very interesting and acceptable result. These errors happens due to different error sources such as bonding inaccuracy, soldering defect, material inhomogeneity, alignment problem and manufacturing inaccuracy. It is believed that all these mentioned error sources can be minimized by applying accurate method and

using skilled personals for the installation and manufacturing of the sensor and the errors could be minimized further.

Manufacturing Cost Estimation

Materials

- Mechanical structure: (two plates of aluminum with 180mmx130mmx1.5mm) with a total price of 4US$
- 12 Strain gauges: (Hottinger, Germany) with a price of 8 US $ each: which means a total of 96 US$
- Tooling: (bending and milling) 8hoursx1US$/hr = 8 US$
- Application of strain gauges: 8 hoursx0.5US$/hr =4 US$
- Wiring: 8 hoursx0.5US$/hr =4 US$
- Assembling: 1 hoursx0.5US$/hr = 0.5US$
- Calibration: 3 daysx4US$/day =12US$

Total manufacturing cost = 128.5 US$

CHAPTER FIVE

CONCLUSION AND FUTURE WORK

5.1 Conclusion

This study describes the design, fabrication and testing of a new six component force and moment sensor. The sensor body is manufactured from aluminum with a rectangular box like structure and its sensing elements are designed based on the conventional bending beam theory. It has a very simplified shape compared with previous designs. As a result, it can be manufactured easily with the minimum cost. The sensor is tested and the result showed that F_x is measured with 70.5%, F_y is measured with 60.9%, F_z is measured with 77.5%, M_x is measured with 63.7%, M_y is measured with 64.8% and finally M_z is measured with 66.1% accuracy. The sensor can also measure each force or moment independently without changing the measuring setup so that it minimizes measuring time. As a result it can conclude that the developed six component force/moment sensor can be used to measure aerodynamic loads in wind tunnel and in robotic system.

5.2 Future Work

The test results presented during the experiment of this study are obtained by applying each force/moment independently. This is because the strain indicator used in the experiment can display only one bridge output at a time. Therefore it requires additional five strain indicators to display the results of the whole bridges simultaneously. However, instead of using strain indicator it is also

possible to design a microprocessor which can process the strain signal and interface with a computer. So the following are recommended as a future work of for the extension of this study.

- Designing microprocessor for six component force /moment sensor
- Finite element analysis and developing a computer program for the six component force /moment sensor
- Developing a method to calibrate the six component force /moment sensor

References

1. Gab-Soon Kim, “The design of a six-component force/moment sensor and evaluation of its uncertainty’’, Measurement Science and technology, 2001.
2. Gab-Soon Kim, “The design of a small six-axis force/moment sensor for robot’s fingers”, Measurement Science and technology, 2004.
3. Farhad A., Martin B., John M. Hollerbach. “Design of a hollow hexaform torque sensor for robot joints”, The International Journal of Robotics Research Vol. 20, No. 12, pp. 967-976, December 2001.
4. V.D. Scheiman, “A preliminary work on implementing a manipulator force sensing Wrist, AI Laboratory Report, Stanford University, 1971.
5. Lincoln P. Erm and Phil Ferrarotto, “Development of a five-component strain-gauge balance for the DSTO water tunnel, DSTO-GD-0597, Platforms Sciences Laboratory, Defense Science and Technology Organization, Melbourne, Australia, 2009.
6. Marin SANDU, Adriana SANDU and Georgeta IONACU, “Design of a compact six-component force and moment sensor for aerodynamic testing”, INCAS BULLETIN, Volume 3, pp. 95 – 100,Issue 1/ 2011.
7. Dr. Rer. Nat. G. Schewe, “Force and Moment Measurements in Aerodynamics and Aero elasticity Using Piezoelectric Transducers” Springer Handbook of Experimental Fluid Mechanics, 2007.
8. Zhaolin Fan, “Measurement of Aerodynamic Forces and Moments in Wind Tunnels”, China Aerodynamics Research and Development Center, Mianyang, Sichuan, China, John Wiley & Sons, Ltd. 2010.
9. Sheng A. Liu and Hung L. Tzo, “A novel six-component force sensor of good measurement isotropy and sensitivities”, Sensors and Actuators A 100 (2002) 223–230.
10. Farhad A., Martin B., John M. Hollerbach. “Design of a hollow hexaform torque sensor for robot joints”, The International Journal of Robotics Research Vol. 20, No. 12, December 2001, pp. 967-976.
11. L.P. Chao, K.T. Chen, Shape optimal design and force sensitivity evaluation of six-axis force sensors, Sens. Actuat. A 63 (1997) 105–112.

12. Chul-Goo kang, ‘’Maximum Structure Error Propagation of Multi-axis Force Sensor’’, JSME International Journal, Series C, Vol. 44, No. 3, 2001.
13. Timm Preusser and Lubomir Polansky, “External 6-component wind tunnel balances for aerospace simulation facilities”, Carl Schenck AG, Industrial Weighing Division, IEEE 1989.
14. Yabuki A, “Six-axis force/torque sensor for assembly robots Fujitsu Sci. Technol. J. 26 41–7, 1990.
15. Hatamura Y et al, “A miniature 6-axis force sensor of multi-layer parallel plate structure IMEKO 567–82, 1989.
16. Makoto Kaneko: “Twin Head Six-Axis Force Sensors”, IEEE Transactions on Robotics and Automation, Vol. 12, No.1, February 1996.
17. Makoto Kaneko: “A new Design of Six Axis Force Sensors”, in Proceeding IEEE Int. Conf. Robotics and Automation, 1993, pp. 961-967.
18. Y. K. Rark, R. Kumme, D. Roeske, D. I. Kang, “Column-type multi-component force transducers and their evaluation for dynamic measurement”, Measurement Science and Technology, vol. 19, pp. 1-10, 2008.
19. A. Sandu, M. Sandu, C. Atanasiu, “A low-profile sensor for six force/torque components”, pp. 67 69, Proceedings of the 18th DANUBIA-ADRIA Symposium on Experimental Methods in Solid Mechanics, Steyr, Austria, September 26-29, 2001.
20. M. Sandu, A. Sandu, “Analytic-numerical approach in a multicomponent strain gauge transducer design”, Scientific Bulletin of University POLITEHNICA of Bucharest, vol. 67, no. 3, pp. 37- 44, 2005.
21. Shengmei Wang, “Design and Developmental Studies On a six-degree of Freedom Endoscopic Force/Torque Sensor”, MSc. Thesis, Concordia University, Montreal, Quebec Canada; 2003.
22. F. Beyeler, S. Muntwyler, Z. Nagy, M. Moser, B. J. Nelson, “A Multi-Axis MEMS Force-Torque Sensor for Measuring the Load on a Microrobot Actuated by Magnetic Fields”, IEEE/RSJ International Conference on Intelligent Robots and Systems, Oct 29 - Nov 2, 2007.
23. Felix Beyeler, Simon Muntwyler, and Bradley J. Nelson, “A Six-Axis MEMS Force–Torque Sensor with Micro-Newton and Nano-Newton meter Resolution” Journal of Micro Electromechanical Systems, Vol. 18, NO. 2, April 2009.